Beni-Suef University Journal of Basic and Applied Sciences

RESEARCH

Open Access

# Solubility enhancing lipid-based vehicles for artemether and lumefantrine destined for the possible treatment of induced malaria and inflammation: in vitro and in vivo evaluations

Onyinyechi Lydia Ugorji[1*], Ikechukwu Virgilius Onyishi[1], Julie Ngozichukwuka Onwodi[1], Christiania Moji Adeyeye[2], Uzochukwu Gospel Ukachukwu[3] and Nicholas Chinedu Obitte[1]

## Abstract

**Background** The lipid self-emulsifying system has been advanced as a promising delivery vehicle for improving the solubility and bioavailability of artemether and lumefantrine. However, the observed kinetic instability (propensity of lumefantrine to rapid crystallisation from nano-scale droplets) in aqueous acid has impelled some researchers to incorporate surfactants/solubilizers in the dissolution medium prior to dissolution studies. Thus, in our present work, we sought to prepare micro/large nano-scale (> 100 nm) and yet kinetically stable lumefantrine lipid self-emulsifying system (that would not require an external drug dissolution enhancing agent in the dissolution medium) and palm kernel oil-based 100 nm kinetically stable artemether lipid self-emulsifying system with rapid emulsification time. COVID-19 and *Plasmodium falciparum*-infected Africans with previous long exposure to malaria have manifested attenuated inflammatory cytokines more than malaria-naive patients. Therefore, the ingestion of artemether-lumefantrine with enhanced solubility may further promote blunting of cytokines. Therefore, this work was aimed at preparing (< 100 nm) stable artemether and aqueous acid-stable micro/large nano-scale (> 100 nm) lumefantrine lipid self-emulsifying system destined for improved antimalarial and anti-inflammatory activities.

**Results** The droplet sizes of all the liquid artemether and lumefantrine formulations were between 8.95–39.88 and 1018–4195 nm, respectively. The loading efficiency for all the formulations was, between 72.91 ± 2.89 and 100.00 ± 0.29%. All the artemether and lumefantrine batches emulsified within the range of 3.90 ± 0.69 to 12.26 ± 0.69 s. Stable and transparent emulsions were formed on aqueous dilution to 1000 ml. The percentage drug released for artemether and lumefantrine ranged from 76.25 ± 2.98 to 99.22 ± 1.61%. The solid lipid self-emulsifying systems produced, had fair and passable flow properties. Differential scanning calorimetry revealed that the solid artemether and lumefantrine lipid self-emulsifying system were amorphous. Solidification with Neusilin $FH_2$ or surfactant replacement with Kolliphor EL and Kollidon VA 64 fine prevented micro-or large nano-scale lumefantrine lipid self-emulsifying system from crystallisation in aqueous acid (pH 1.2). Higher antimalarial activity and remarkable anti-inflammatory effects ($P < 0.05$) favoured the lipid self-emulsifying formulations.

*Correspondence:
Onyinyechi Lydia Ugorji
Lydia.ugorji@unn.edu.ng
Full list of author information is available at the end of the article

**Conclusion** Optimal in vitro and in vivo results (enhanced antimalarial and anti-inflammatory activities) were obtained with kinetically stable lumefantrine micro/large nano-scale droplets and kinetically stable palm kernel oil-based (< 50 nm) artemether lipid self-emulsifying system droplets.

**Keywords** Lipid self-emulsifying system (LSES), Artemether (ART), Lumefantrine (LUM), Neusilin $FH_2$, Anti-malarial, Anti-inflammatory

## 1 Background

The water solubility of more than 75% of the chemicals currently being developed is poor. The bioavailability of medications that are poorly aqueous soluble following oral administration is likely to be low due to the difficulties in disintegrating and dissolving in the gastrointestinal system. Recently, lipid-based drug delivery systems like lipid self-emulsifying systems (LSES) have gained increasing attention for the past decade by virtue of improving the oral bioavailability of poorly water-soluble or lipophilic drugs. Recent researches have reported the use of lipid-based systems to improve the solubility, bioavailability and wide range of therapeutic activities [1–3]. LSES is a mixture of lipid, surfactant, and co-solvent/co-surfactant with isotropic characteristics, which emulsifies spontaneously to produce a fine oil-in-water or water-in-oil emulsion under gentle agitation in the aqueous phase [4–6]. The advantages of emulsions include high drug loading capacity, reduced drug irritation/toxicity, protection of sensitive drugs, improved drug dissolution, enhanced absorption and bioavailability [4, 7]. The complementary effects of oil and surfactant provide a solubilising milieu that forms dispersions of less or greater than 100 nm in the aqueous phase [8–10].

Artemether (ART) and lumefantrine (LUM), the model drug candidates deployed in this work, are WHO-approved antimalarial combination therapy molecules with poor aqueous solubility [11]. When orally administered, their dissolution rate in the gastrointestinal tract becomes the rate-limiting step to absorption [12, 13]. Their low aqueous solubility and concomitant poor bioavailability may result in poor therapeutic outcomes. The most worrisome is the possibility of initiating drug resistance caused by sub-lethal tissue drug concentration [14, 15]. The lipid self-emulsifying system can address these challenges. In addition to its antimalarial properties, the promising anti-inflammatory and immunomodulatory potential of ART has been documented [16]. Different types of inflammation may be the outcome of viral infections. SAS-COV-2 is known to cause an intense inflammatory cytokine storm [17, 18]. Africans who have previously had long exposures to malaria (and, of course, antimalarial drugs) have shown fewer COVID-19-based inflammatory cytokines compared to malaria-naive individuals with null or lower exposures [19]. Therefore, the ingestion of ART-LUM with enhanced solubility may further promote blunting of cytokines and perhaps explain the reduction in mortality rate among Africans on COVID-19 comorbidity therapy.

Despite the promising potential of LSES, reports have shown that in the presence of surfactants, oleic acid (OA) dissolves LUM more than most oils because of the hydrophobic ionic complexation interaction between anionic OA and cationic LUM [20]. However in the presence of aqueous acid, which has a stronger ionic strength, the OA-LUM bond is broken, resulting in precipitation. This precipitation challenge may have informed the exclusion of SGF/0.1N HCl as a dissolution medium for ART-LUM Self-Nano-Emulsifying Drug Delivery System (SNEDDS) by some workers [14]. To improve dissolution, they only used phosphate buffer pH 7.2, which was modified with 1% sodium lauryl sulfate. A previous researcher conducted in vitro release studies on ART-LUM nano-liposomes using only pH 7.2 dissolution medium [21]. Another researcher carried out dissolution studies on LUM nano-powder using 0.1N HCl containing 0.1–1% w/v benzalkonium chloride solution [22]. In previous clinical studies, conventional LUM tablets and LUM solid dispersion required co-administration with 365.8 kcal and 497 kcal of fat, respectively, to achieve enhanced solubilisation and bioavailability of LUM [23, 24]. To the best of our knowledge, there is paucity of data on the investigation of micro/large nano-scale LUM LSES droplets with kinetic stability in aqueous acid that do not require the incorporation of surfactants/solubilizers in the dissolution medium prior to dissolution studies. Furthermore, due to the reported anti-inflammatory and immunomodulatory potential of ART, we embarked on a preliminary investigation on the anti-inflammatory properties of the ART/LUM LSES with enhanced solubility. A positive outcome may motivate further studies to understand the role of ART/LUM LSES in the management of COVID-19-associated inflammations in patients simultaneously suffering from malaria.

In our present work, we produced acid-stable micro/large nano-scale droplets of LUM LSES with short emulsification time as preferred alternatives to LUM nanocrystals and nanodroplets susceptible to crystallisation in aqueous acid, and ART LSES using vegetable oil (palm kernel oil)(PKO) due to their GRAS status,

biocompatibility, cost-effectiveness, and availability [4, 25]. Therefore the aims of this study was to create stable PKO-based nano-scale (50 nm) ART LSES and aqueous acid-stable OA-based micro/large nano-scale (> 100 nm) LUM LSES with enhanced anti-inflammatory and antimalarial activities.

## 2 Experimentals

### 2.1 Materials

Shea butter was procured from Owode market Offa, Kwara– State Nigeria, Palm kernel oil (locally sourced from Ogige market, Nsukka, Nigeria), Oleic acid (Nasfco Scientific Supplies Ltd, London), Tween 80 (Sigma Aldrich, Germany), Kolliphor EL, Kolliphor RH 40, Kolliphor HS 15, Kollidon VA 64 (BASF, Germany), Labrasol, Gelucire, Lauroglycol 90, Lauroglycol FCC, Capryol 90, Capryol pgmc, Peceol, Labrafac lipophile (Gift samples from Gattefosse, France), Artemether (Hangzhou Dayang chemical, China), Lumefantrine (Hangzhou Dayang chemical, China), Neusilin FH2 (Fuji Chemical Industry Co. Japan), Hydrochloric acid (Sigma Aldrich, Germany), Absolute Methanol(Sigma Aldrich, Germany), Distilled water (STC Unit UNN). All other chemicals are of analytical grade and were used as such.

### 2.2 Purification of oils

A 2% w/w suspension of a 2:1 ratio of activated charcoal and bentonite mixture in shea butter or palm kernel oil was heated at 80–90 °C for 1 h and filtered using Whatman filter paper [13].

### 2.3 Solubility studies

An excess amount of artemether was added to each of the excipients (lipids, surfactant, co-surfactant) and agitated with a mechanical flask shaker at intervals for 24 h. A 0.1 ml volume of the supernatant was withdrawn from each sample and introduced into a 100 ml volumetric flask containing 25 ml of 1N HCl. It was heated for 20 min at 80 ± 2 °C, cooled, and made up to 100 ml with distilled water. At a wavelength of 325 nm, the amount of artemether and thus its solubility in various excipients were determined spectrophotometrically (UV/VIS Spectrulab UK). The procedure above was followed for the solubility studies of lumefantrine. 0.1 ml of the supernatant was mixed with 70 ml of 0.1 M methanolic HCl in a 100 ml volumetric flask. The volume was made up to 100 ml with 0.1 M methanolic HCl and labelled as the stock solution. From the stock solution, 1 ml was taken and made up to 10 ml with methanolic HCl, and the solubility values were determined spectrophotometrically at a wavelength of 335 nm [8]. Triplicate determinations were made.

### 2.4 Pseudoternary phase studies

The pseudoternary phase diagrams were developed by the water titration method. Aliquots of each surfactant, co-surfactant and oil were mixed together at room temperature. The surfactant and co-surfactant (Smix) were mixed according to these ratios: 1:0, 1:0.5, 1:1, 1:2, 1:3, 3:1, and 3:2. Then the ratio of oil to Smix was varied as follows: 1:9, 1:8, 1:7, 1:6, 1:5, 1:4, 1:3.5, 1:3.0, 1:2.5, 1:2.0, 1:1.5, 1:1, and 1:0.5. Drop-wise quantities of water were added to each oil–smix mixture and mildly shaken until the end point was reached. The ratios that gave stable LSES were then selected.

### 2.5 Formulation of LSES

Drug-loaded anhydrous LSES was prepared based on stable batches arising from pseudo-ternary phase diagrams. An 80 mg quantity of artemether was added to appropriate quantities of palm kernel oil, Kolliphor HS 15: Tween 80 (1:1), and Capryol PGMC® (Table 1). The mixture was mixed under magnetic stirring (Gallenkamp, England) to give a final concentration of 80 mg of artemether per 800 mg of LSES formulation. The 50 mg of lumefantrine per gram of LSES was also prepared by stirring a mixture of lumefantrine (50 mg), oleic acid, Kolliphor HS 15, and Capryol PGMC® (Table 1). For further studies, the formulations were stored at an ambient temperature of 30 ± 0.5 °C.

### 2.6 Centrifugation test/stability test

The anhydrous drug loaded emulsions with different concentrations of artemether and lumefantrine were stored for 72 h at room temperature and observed for isotropicity (homogeneity, phase separation and drug precipitation). The formulations were subsequently centrifuged at 3500 rpm for 15 min using a centrifuge (Uniscope, England) and observed for the above-mentioned changes.

### 2.7 Freeze and thaw cycle test

The anhydrous drug-loaded emulsion was visually assessed after 72 h of storage at 30 ± 0.5 °C. Fresh samples were stored in a refrigerator at 4 °C for 12 h, and thereafter they were subjected to an ambient temperature of 30 °C for 12 h. This cycle was repeated daily for 3 days and observed for drug precipitation and phase separation.

### 2.8 Emulsification time and aqueous dilution test

The emulsification time of the formulations was determined by introducing a unit dose into a 250 ml beaker containing 100 ml of 0.1N HCl for artemether LSES or 100 ml of phosphate buffer solution (pH 7.2) for

**Table 1** Composition of artemether and lumefantrine loaded LSES

| i. Formulation code | A1:0.5 | B1:0.5 | C1:0.5 | A3:1 | B3:1 | C3:1 |
|---|---|---|---|---|---|---|
| O:S:C | 23:51:26 | 16:56:28 | 15:57:28 | 23:58:29 | 16:63:21 | 11:66:23 |
| Palm kernel oil (mg) | 187.44 | 129.44 | 120.24 | 185.04 | 123.52 | 68.32 |
| Solutol: Tween 80 (mg) | 204.2: 204.2 | 223.52: 223.52 | 226.6: 226.6 | 230.6: 230.6 | 253.68: 253.68 | 274.36: 274.36 |
| Capryol pgmc (mg) | 204.16 | 223.52 | 226.56 | 153.76 | 169.12 | 182.96 |
| Artemether (mg) | 80 | 80 | 80 | 80 | 80 | 80 |
| **ii. Formulation code** | **A3:1** | **B3:1** | **C3:1** | **A3:2** | **A1:0.5** | **B1:0.5** |
| O:S:C | 32:49:19 | 39:45:17 | 24:57:19 | 31:41:23 | 30:47:23 | 22:52:26 |
| Oleic acid (mg) | 298.4 | 361.6 | 241 | 308.1 | 298.3 | 215.9 |
| Solutol (mg) | 526.4 | 478.8 | 569.25 | 415.14 | 407.8 | 522.7 |
| Capryol pgmc (mg) | 175.4 | 159.6 | 189.75 | 276.76 | 233.9 | 261.4 |
| Lumefantrine (mg) | 50 | 50 | 50 | 50 | 50 | 50 |

*O* oil, *S* surfactant, *C* co surfactant

lumefantrine. This alkaline pH was preferred because LUM precipitated in 0.1N HCl medium [13]. The beaker was placed on a hot plate–magnetic stirrer (Gallenkamp, England) assembly, set at 100 rpm and a temperature of 37 ± 0.5 °C. The time for complete emulsification was observed and recorded. Triplicate determinations were made. A 400 mg quantity of artemether or LUM LSES was emulsified in 100 ml of 0.1 N HCl or phosphate buffer pH 7.2 and diluted further to 1 L. Each was stored for 5 h, 24 h, and 1 week, respectively, and observed for drug precipitation.

### 2.9 Particle size analysis and polydispersity index test

Particle size and polydispersity index were determined using a zeta sizer (Malvern Instruments, UK) at a light scattering angle of 90° [4]. Triplicate determinations were made.

### 2.10 Preparation of solid and liquid acid-stable LSES

To forestall crystallisation of LUM from the above LSES in aqueous acid, solidification or surfactant replacement and crystallisation inhibitor inclusion were carried out. The liquid LSES was mixed with ethanol (96%) at 4:3 ratios and blended with Neusilin $FH_2$ at a Neusilin to LSES ratio of 6:4 and screened through sieve No 14 (Endecotts UK). The mass was air dried at room temperature before being oven dried for 1 h at 40 °C. The solid LSES was then screened through the same sieve and subsequently evaluated for bulk and tapped density, compressibility index, flow rate, angle of repose and other powder properties [26, 27]. Artemether solid LSES was also prepared as above. A 1 g quantity of solid ART LSES containing 40 mg of artemether or a 2.5 g quantity of LUM containing 50 mg of LUM was filled into size 0 capsules. To confer aqueous acid-stability on LUM LSES, Kolliphor HS 15 was replaced with Kolliphor EL, while Capryol® PGMC was replaced with Lauroglycol® 90. In brief, LUM was mixed with oleic acid, Kolliphor EL, and Laurogylcol® 90 and stirred with a magnetic stirrer to achieve a final concentration of 60 mg of LUM per g of LSES. Thereafter, 100 mg of Kollidon VA 64 fine, a crystallisation inhibitor and dispersant, was introduced into the mixture and stirred until it completely dissolved (Table 2). Subsequently, the liquid formulations were evaluated for loading efficiency, droplet size, polydispersity index, emulsification time, and aqueous dilution as earlier described.

**Table 2** Composition of Lumefantrine LSES using Kolliphor EL as surfactant component

| Ratio (O:S:C) | Oil (oleic acid) ml | Surfactant (kolliphor EL) ml | Co-surfactant (lauroglycol) ml | Kollidon VA 64 (mg) |
|---|---|---|---|---|
| 34:50:16 | 0.34 | 0.41 | 0.16 | 100 |
| 34:55:11 | 0.34 | 0.45 | 0.11 | 100 |
| 34:60:04 | 0.34 | 0.49 | 0.06 | 100 |
| 34:65:01 | 0.34 | 0.54 | 0.01 | 100 |

### 2.11 Drug content/loading efficiency of the LSES

Unit dose of each artemether or lumefantrine formulation was assayed as described under solubility studies. From the drug content, the % loading efficiency was calculated as below:

$$\%\ \text{Drug loading efficiency} = \frac{\text{Drug content}}{\text{Amount of drug incorporated}} \times 100 \quad (1)$$

### 2.12 Drug release studies

The dialysis and basket (Apparatus I) methods were, respectively, adopted to study the dissolution behaviour of the formulations. Before use, the cellulose membrane was presoaked in the medium (SGF, pH 1.2 or Phosphate buffer, pH 6.8) for 24 h. A mixture of 0.4 ml of the LSES (equivalent to 40 mg of artemether) and 1 ml of the medium was introduced into a 6 cm long membrane tied at both ends. This was subsequently tied to a vertical spindle and lowered into a 500 ml beaker containing the dissolution medium and positioned on a magnetic stirrer (Gallenkamp, England). The volume of dissolution medium used was 500 ml and the stirrer rotation speed was 100 rpm, while the temperature was maintained at 37 ± 0.5 °C. At a predetermined interval (0, 0.5, 1, 2, 3, 4, 5, 6 h), 5 ml aliquots of the dissolution medium were sampled and replaced with 5 ml of the corresponding fresh medium. The samples were treated as earlier described and assayed spectrophotometrically for artemether. Triplicate determinations were made. The assay procedure above was carried out on lumefantrine LSES (equivalent to 50 or 60 mg of drug) using methanolic HCl and spectrophotometrically assayed for the amount of lumefantrine present as previously described. Dissolution studies were also carried out using the basket method (apparatus I) at time intervals was 0, 2, 5, 10, 15, 20, 25, 30, 35, 40, 45 min [4].

### 2.13 Differential scanning calorimetry (DSC) on solid LSES

Thermal analysis as well as excipient compatibility was studied using differential scanning calorimetry. The DSC (Netzsch DSC 204 F1, Germany) of solid LSES and Neusilin FH2 was measured at temperatures ranging from 50 to 350 °C. The analysis was performed under a liquid nitrogen atmosphere at a rate of 10°/min.

### 2.14 Antimalaria studies

The formulations with the least particle sizes and high drug loading efficiency were chosen for the in vivo studies. *The Plasmodium berghei* parasites were obtained from the National Institute of Medical Research, Lagos, Nigeria. Peter's 4-day suppressive test was adopted [28, 29]. Earlier before the animal experiment, the Animal Ethics Committee at the Faculty of Pharmaceutical Science, University of Nigeria, Nsukka approved the research protocol for the use of experimental animals. Hence, the study was conducted in accordance with the Ethical Guidelines of the Animal Care and Use Committee (Research Ethics Committee) of the University of Nigeria, Nsukka, following the Federation of European Laboratory Animal Science Association and the European Community Council Directive of November 24, 1986 (86/609/EEC) [4]. A 0.2 ml quantity of donor mouse blood diluted with Phosphate buffer saline (PBS) containing parasitized erythrocytes was intraperitoneally inoculated into 15 groups of 6 Swiss albino mice per group, which weighed between 20 and 30 g (parasetamia level, 27–35%). The groups are as follows:

Group A treated with solid ART LSES.
Group B treated with solid LUM LSES.
Group C treated with solids ART-LUM LSES.
Group D was given liquid ART LSES.
Group E treated with liquid LUM LSES.
Group F was given ART-LUM liquid LSES.
Group G treated with crushed commercial ART-LUM tablet.
Group H was given palm kernel oil-based LSES without ART (as a control).
Group I treated with distilled water (control).
Group J was given oleic acid-based LSES without lumefantrine (as a placebo).
Group K received solid LSES based on Neusilin without artemether (placebo).
Group L received solid LSES based on Neusilin without lumefantrine (placebo).
Group M was given an aqueous dispersion of ART.
Group N treated with an aqueous dispersion of LUM.
Group O was given an aqueous dispersion of LUM-ART.

Treatment was initiated daily from day 0 through day 3 with 4 mg/kg of artemether and 24 mg/kg of lumenfantrine, respectively. On the fourth day, blood was taken from the mice and thinly smeared on a microscope slide. The blood films were fixed on the slide using methanol and stained with Giemsa, pH 1.2. The number of parasitized erythrocytes was recorded after counting 250 red blood cells from each slide. This is how antimalarial activity was calculated [30].

$$\text{Activity} = 100 - \frac{\text{mean parasitemia of treated group}}{\text{mean parasitemia of control}} \times 100 \quad (2)$$

### 2.15 Preliminary anti-inflammatory studies

Sheep red blood cells (SRBC) were sourced from Obollo afor Abbatoir, Nsukka, Nigeria. The cells were washed thrice in copious volumes of normal saline by centrifugation at 5000 rpm for 10 min. The supernatant was aspirated and the packed cells were adjusted to a concentration of $1.0 \times 10^8$ cells/ml with chilled normal saline. Mice were induced to inflammation by injecting 0.1 ml of 25% v/v SRBC in normal saline intraperitoneally. The

SRBC-induced mice were divided into nine groups, each consisting of five mice per group. Control groups received distilled water, diluents, and standard drug solutions. Artemether (40 mg/kg), Lumefantrine (40 mg/kg) and drug-loaded LSES formulations were administered orally to the mice for 5 days consecutively as described below.

| | |
|---|---|
| Group 1 | SRBC + distilled water |
| Group 2 | SRBC + oleic acid and palm kernel oil LSES |
| Group 3 | SRBC + commercially ART-LUM tablet |
| Group 4 | SRBC + aqueous dispersion of ART &LUM |
| Group 5 | SRBC + aqueous ART dispersion |
| Group 6 | SRBC + aqueous LUM dispersion |
| Group 7 | SRBC + artemether + lumefantrine LSES |
| Group 8 | SRBC + artemether LSES |
| Group 9 | SRBC + lumefantrine LSES |

The anti-inflammatory activities of the mice were investigated by determining the haemagglutination antibody (HA) titre, delayed type hypersensitivity (DTH), and white blood cell differentials. The procedures are described below.

### 2.16 Haemagglutination antibody (HA) Titre

Each mouse was immunized intraperitoneally with 0.1 ml of 25% v/v SRBC in normal saline on day 0. Blood samples were collected through the orbital plexus from each animal on day 7, and the antibody titre was determined by a modified haemagglutination technique [31]. In eppendorf tubes, two-fold diluted sera in phosphate buffered saline (PBS) pH 7.2 (25 µl) were mixed with 25 µl of 1% SRBC suspension in PBS (pH 7.2). The tubes were incubated at 37 °C for 1 h and monitored for haemagglutination. Antibody titre was measured by observing a value with the highest serum dilution that showed visible haemagglutination.

### 2.17 Delayed type hypersensitivity (DTH)

DTH was evaluated as described. On day 14, the mice were again challenged with 0.1 ml of 25% v/v SRBC suspension in normal saline at the left-hind foot pad. After 24 h, the thickness of the left-hind foot pad was then measured using a vernier caliper. The difference between the thickness of the left hind foot pad and the right hind foot pad was used as the DTH index [32].

### 2.18 White blood cell differentials

The white blood cell differential was done using a compound light microscope (GXM-F2000, Olympus-UK). Drops of peripheral blood samples were collected on day 14 from the tails of the mice and were used to make smears on glass slides and allowed to dry [33]. The dried smears were fixed and stained using rapid-stain kit reagents following the protocol described in the rapid-stain kit manual (Antigënes, Germany), and then viewed under the light microscope at a magnification of 100 X aided by an immersion oil. 100 leukocytes were counted per slide and their observed percentage differentials were noted.

### 2.19 Histopathology studies

The histopathological study was conducted in accordance with the Ethical Guidelines of the Animal Care and Use Committee (Research Ethics Committee) of the University of Nigeria, Nsukka, following the Federation of European Laboratory Animal Science Association and the European Community Council Directive of November 24, 1986 (86/609/EEC) [4]. A 0.2 ml quantity of donor mouse blood containing parasitized erythrocytes was diluted with phosphate buffer saline (PBS) and intraperitoneally inoculated into 5 groups of 5 Swiss albino mice per group, which weighed between 15 and 20 g. The groups are as follows: Group A was treated with normal saline (control); Group B was infected and treated with ART-LUM (ART, 2 mg/kg body weight and LUM, 12 mg/kg body weight) as a low dose; Group C was infected and treated with ART-LUM (ART, 4 mg/kg body weight and LUM, 24 mg/kg body weight) as a normal/medium dose; Group D was infected and treated with ART-LUM (ART 8 mg/kg body weight and LUM 48 mg/kg body weight) as a high dose; Group E was infected and untreated. The drugs were administered twice daily for 3 days. Following treatment with the drugs, mice were allowed to fast overnight, sacrificed, and the internal organs such as the spleen, liver, and kidney were collected for histopathology. The liver, kidney, and spleen were fixed in 10% formalin before being dehydrated in increasing concentrations of ethanol [34]. Thereafter, the tissues were soaked in chloroform overnight, infiltrated with, and embedded in molten paraffin wax. The blocks were later trimmed and sectioned at 5–6 microns. The sections were deparaffinized in xylene, immersed in distilled water, and subsequently stained with haematoxylin and eosin (H and E) for light microscopy. Histopathological imaging and assessment were performed under high magnification (400×) (Weltzlar, Germany). The severity level of each histopathological change was graded on a scale of 0–3, according to a semi-quantitative assessment [34, 35].

### 2.20 Data and statistical analysis

Results were expressed as the mean ± standard deviation. All statistical calculations were done with the Sigma Plot

11 software and Graph Pad Instat Demo. *P* values less than 0.05 were considered significant.

## 3 Results

### 3.1 Purification of oils

The purified palm kernel oil and shea butter were all free of odours and debris. They also showed better organoleptic properties compared to the unpurified samples.

### 3.2 Solubility studies

The solubility values of ART and LUM in various excipients are shown in Figs. 1 and 2. LUM recorded the highest solubility (336.8 mg/ml) in oleic acid; on the other hand, ART had the highest solubility in palm kernel oil, hence their choice as the oil phase.

### 3.3 Pseudoternary phase studies

A mixture of palm kernel oil, Tween 80, Kolliphor HS 15 (1:1), and Capryol PGMC were used for the pseudo ternary phase studies to determine the optimal component mixture and delineate the self-emulsifying region for artemether LSES. Kolliphor HS 15 was previously used as the surfactant component. However, because of its low miscibility with water and small self-emulsifying

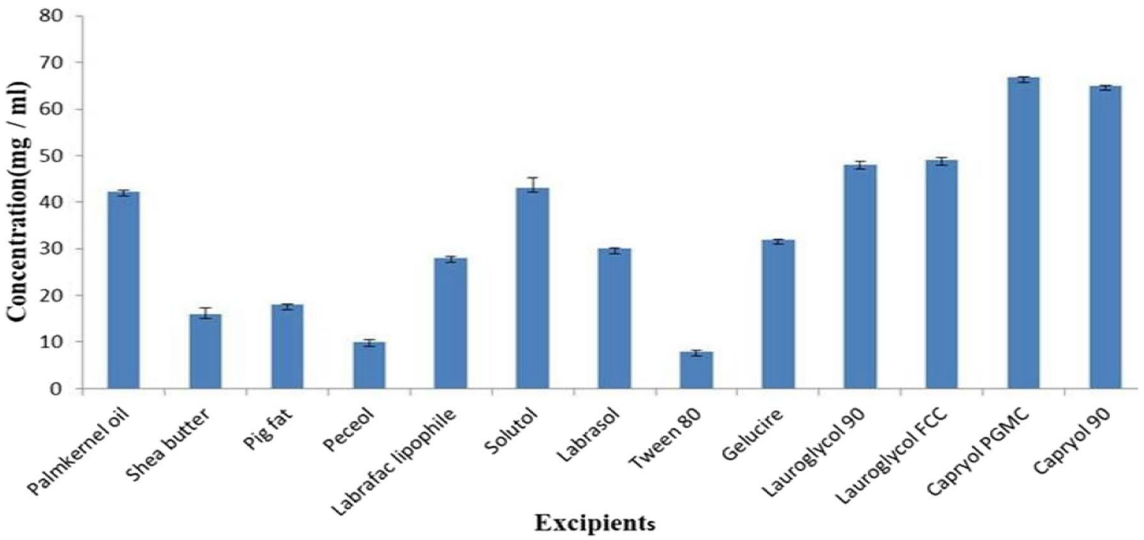


**Fig. 1** Bar chart presentation of the solubility of artemether in various excipients

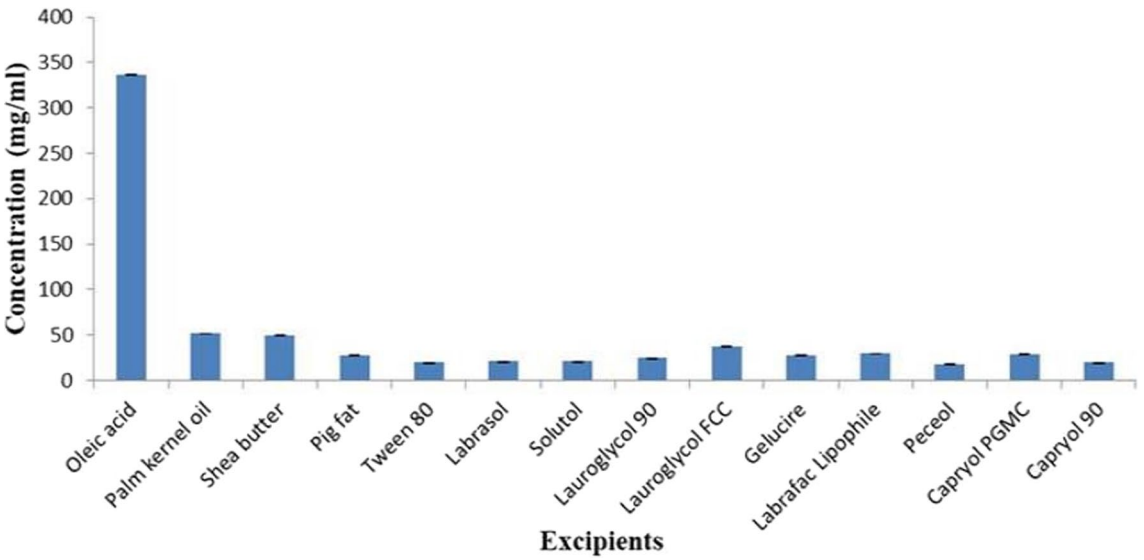


**Fig. 2** Bar chart representation of the solubility of lumefantrine in various excipients

domain, it was blended with Tween 80 at a ratio of 1:1. On the other hand, a mixture of oleic acid (oil), Kolliphor HS 15 (surfactant) and Capryol PGMC (co-surfactant) was used for the pseudo ternary phase studies of lumefantrine LSES. Large areas of self-emulsification were obtained at Smix (surfactant: co-surfactant) ratios of 1:0.5 and 3:1 (Figs. 3, 4) for both lumefantrine and artemether. In additional pseudoternary phase studies where the Kolliphor HS 15 was replaced with Kolliphor EL, large areas of self-emulsification were obtained at Smix ratios of 1:3 and 3:1.

### 3.4 Post-formulation isotropicity/centrifugation test/ astability test and freeze and thaw cycle test

The LSES batches were visually transparent, which evidences complete excipient miscibility and drug solubilisation. There was no observed instability following the refrigeration cycle and centrifugation tests.

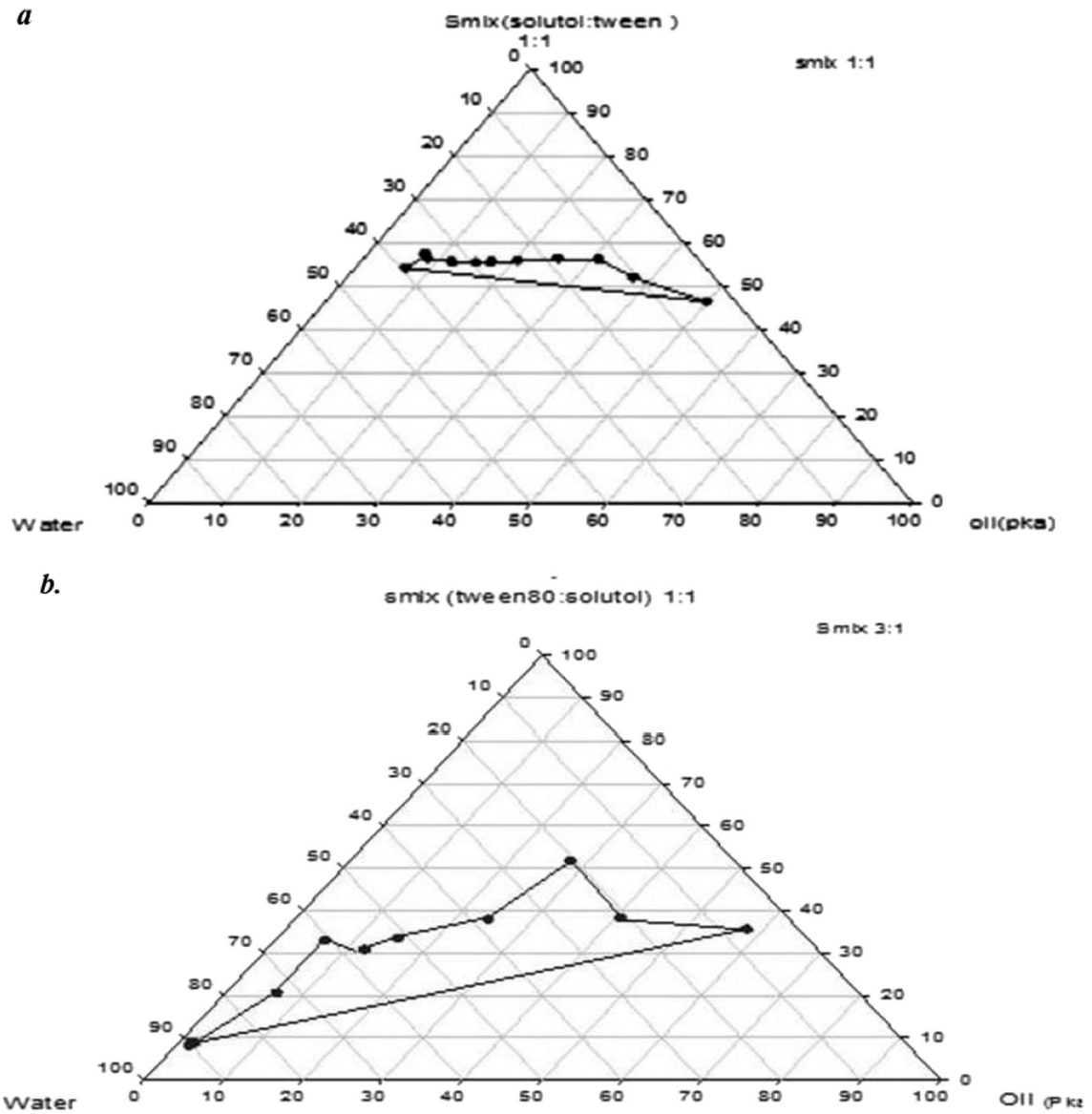


**Fig. 3** **a, b** Pseudoternary phase diagram consisting of palm kernel oil, Solutol and Tween 80 (1:1) at **a** Smix 1:1 and **b** Smix 3:1. **Smix* surfactant mixture, *pk/pka* palmkernel oil

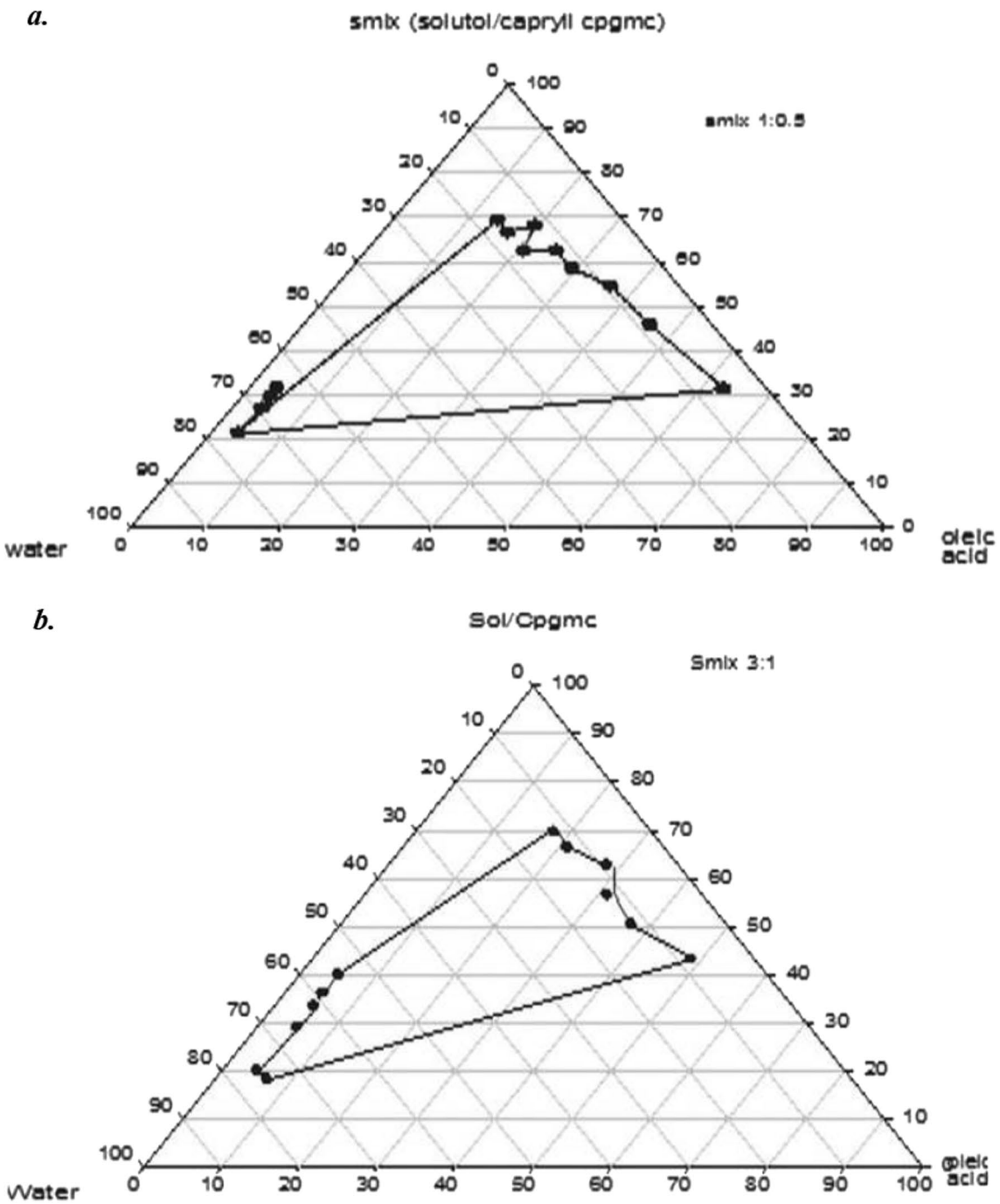


**Fig. 4** **a, b** Pseudoternary phase diagram consisting of oleic acid, Solutol, Capryol pgmc **a** Smix 1:0.5 and **b** Smix 3:1. **Smix* surfactant mixture, *Cpgmc* Capryol pgmc

### 3.5 Emulsification time test and aqueous dilution test

However, in the aqueous phase, Kolliphor HS 15 LUM LSES proved to be kinetically unstable due to precipitation in aqueous acid (though not in phosphate buffer pH 7.2). In SGF, the ART formulations emulsified within 3–8 s to form a clear or bluish microemulsion, while in phosphate buffer solution (pH 7.2), Kolliphor HS 15 LUM LSES emulsified within 6–12 s. On the other hand, Kolliphor EL-based LUM LSES emulsified in SGF pH 1.2 within 91.8–132 s, but upon the inclusion of Kollidon VA 64 fine in the LSES, the ET was reduced to 51–72 s. All the ART batches were clear and transparent on dilution to 1000 ml

with distilled water, except for batch $A_{1:0.5,}$ which was bluish in colour. In storage for 5 h and up to 24 h, they still retained their visual appearance. The Kolliphor HS 15-based LUM batches were also clear, transparent and stable after 5 h following dilution with distilled water, but a cloudy appearance was observed after 24 h of storage. As afore-noted, dilution in SGF pH 1.2 prompted rapid drug precipitation. This was, however, not the case with Kolliphor EL-Kollidon VA 64 fine LUM LSES, which were stable at 5 and 24 h post-dilution in SGF (pH 1.2). Such kinetic stability in the aqueous phase is sufficient to permit the withdrawal of the unit dose prior to oral ingestion. On the other hand, after 5 h dilution, Kolliphor EL LUM LSES (without Kollidon VA 64 fine) developed instability (creaming).

### 3.6 Particle size analysis and polydispersity index test

All the ART formulations showed DS ranging from 8.95 to 39.88 nm with PDI of 0.07–0.25, while Kolliphor HS 15 LUM LSES had DS of 1579–2022 nm and PDI of 0.27–0.33 (Table 3). On the other hand, the DS of Kolliphor EL LUM LSES and Kolliphor EL-Kollidon VA 64 fine LUM LSES ranged from 341.95 to 8493 nm and 504 to 3897 nm, and their corresponding PDI, 0.48–0.8 and 0.7–0.9, respectively. With the exception of Kolliphor EL LSES containing 65% surfactant (34:65:01), the other three batches (34:50:01, 34:55:11, and 34:60:04) had significantly ($P < 0.05$) higher DS than those of Kolliphor HS 15 LSES. However, in spite of their higher DS and PDI, they prevented precipitation of LUM, unlike Kolliphor HS 15 LSES that suffered LUM crystallisation in aqueous acid. Kolliphor EL-Kollidon VA 64 fine LSES with higher PDI provided a better micro-environment that further enhanced the stabilisation of LUM from crystallisation. High PDI may be attributed to irregular molecular interactive adsorption of Kollidon VA 64 fine on the hydrophilic surface of the emulsion droplets.

### 3.7 Granulation properties

The Hausner's quotient (HQ), Carr's compressibility index (CI), angle of repose, and flow rate values of artemether (ART) and lumefantrine (LUM) LSES granulations are shown in Table 4.

### 3.8 Drug content/loading efficiency of the LSES

The loading efficiencies of the liquid and solid ART (LSES) were between 72.91–100 and 62.04–100%, respectively, while those for the liquid and solid LUM LSES ranged between 79.65–96.42 and 86.5–100%, respectively (Table not shown). The loading efficiency of the Kolliphor EL-Kollidon VA 64-based LUM formulation was between 93 and 98%.

### 3.9 Drug release studies and release kinetics

The cumulative amount (%) of ART that diffused through the dialysis membrane into SGF (pH 1.2) or phosphate buffer solution (pH 6.8) was between 76 and 99% or 76 and 100% (Fig. 5a–c), while that of LUM was 9% in SGF (pH 1.2) or phosphate buffer solution (pH 6.8) The apparently poor LUM diffusion from dialysis membrane (molecular weight of 6000 dalton) motivated resort to the use of Apparatus 1 (basket method) for LUM release studies in phosphate buffer solution (pH 6.8). Consequently, the quantity of LUM released was between 84 and 90% (Fig. 5d). Dissolution studies at pH 1.2 were not furthered because of the inadvertent precipitation

**Table 3** Droplet characteristics of the various LSES

| ***Artemether LSES*** | | | | | |
|---|---|---|---|---|---|
| Batch | A1:0.5 | B1:0.5 | A3:1 | B3:1 | C3:1 |
| Droplet size (nm) | 39.88 ± 4.0 | 14.96 ± 6.0 | 14.42 ± 2.5 | 12.10 ± 1.7 | 8.95 ± 0.9 |
| Polydispersity index | 0.25 ± 0.04 | 0.12 ± 0.009 | 0.09 ± 0.002 | 0.11 ± 0.03 | 0.09 ± 0.005 |
| *Kolliphor HS 15 Lumefantrine LSES* | | | | | |
| | 32:49:19 | 30:47:23 | 24:57:19 | | |
| Droplet size (μm) | 1589 ± 104 | 1579 ± 200 | 2022 ± 311 | | |
| Polydispersity index | 0.33 ± 0.068 | 0.34 ± 0.099 | 0.27 ± 0.04 | | |
| *Kolliphor EL Lumefantrine LSES* | | | | | |
| | 34:50:16 | 34:55:11 | 34:60:06 | 34:65:01 | |
| Droplet size (nm) | 8493 ± 778 | 4229 ± 709 | 8852 ± 1395 | 341.95 ± 20.6 | |
| Polydispersity index | 0.64 ± 0.04 | 0.8 ± 0.05 | 0.611 ± 0.2 | 0.48 ± 0.02 | |
| *Lumefantrine + Kollidone VA64 fine LSES* | | | | | |
| | 50 | 55 | 60 | 65 | |
| Droplet size | 3897 ± 1235 | 2228.5 ± 419 | 402.6 ± 85 | 504.6 ± 4.5 | |
| Polydispersity index | 0.9 ± 0.2 | 0.9 ± 0.12 | 0.9 ± 0.008 | 0.7 ± 0.008 | |

**Table 4** Properties of artemether and lumefantrine LSES granules

| Artemether formulation | $A_{1:0.5}$ | $B_{1:0.5}$ | $C_{1:0.5}$ | $A_{3:1}$ | $B_{3:1}$ | $C_{3:1}$ |
|---|---|---|---|---|---|---|
| B.D (g/cm$^3$) | 0.61 ± 0.02 | 0.57 ± 0.01 | 0.58 ± 0.01 | 0.58 ± 0.01 | 0.56 ± 0.01 | 0.55 ± 0 |
| T.D (g/cm$^3$) | 0.81 ± 0.02 | 0.79 ± 0.02 | 0.76 ± 0 | 0.76 ± 0 | 0.72 ± 0.02 | 0.74 ± 0.02 |
| C.I (%) | 25.30 ± 2.0 | 26.91 ± 2.56 | 23.61 ± 1.40 | 23.15 ± 1.6 | 22.04 ± 3.6 | 25.29 ± 2.0 |
| H. Q | 1.34 ± 0.04 | 1.37 ± 0.05 | 1.31 ± 0.02 | 1.30 ± 0.02 | 1.29 ± 0.06 | 1.34 ± 0.03 |
| A.R (°) | 20.62 ± 2.05 | 16.48 ± 0.50 | 21.80 ± 1.0 | 17.82 ± 0.25 | 18.35 ± 1.34 | 19.19 ± 3.03 |
| F.R (g/s) | 7.68 ± 0.45 | 5.89 ± 0.83 | 7.58 ± 0.84 | 7.05 ± 1.39 | 8.55 ± 0.25 | 8.07 ± 0.30 |
| **Lumefantrine formulations** | **$A_{3:1}$** | **$A_{1:0.5}$** | **$C_{3:1}$** | | | |
| *Lumefantrine LSES granules* | | | | | | |
| B.D (g/cm$^3$) | 0.60 ± 0.03 | 0.60 ± 0.03 | 0.58 ± 0.01 | | | |
| T.D (g/cm$^3$) | 0.73 ± 0.04 | 0.75 ± 0.02 | 0.74 ± 0.02 | | | |
| C.I (%) | 17.49 ± 1.45 | 19.41 ± 4.99 | 21.65 ± 3.25 | | | |
| H.Q | 1.21 ± 0.03 | 1.25 ± 0.07 | 1.28 ± 0.05 | | | |
| A.R (°) | 18.34 ± 0.62 | 23.2 ± 0.98 | 23.75 ± 1.18 | | | |
| F.R (g/s) | 7.40 ± 0.21 | 7.37 ± 0.29 | 7.43 ± 0.14 | | | |

Each data is expressed as mean ± SD; n = 3

*B.D* bulk density, *T.D* tapped density, *C.I* compressibility index, *H.Q* Hausner's quotient, *A.R* angle of repose, *F.R* flow rate

of LUM that ensued therein. To address this hiccup, we adopted two approaches: (1) In the LUM LSES, replace Kolliphor HS 15 with Kolliphor EL and Kollidon VA 64. (2) Adsorption of the liquid LUM LSES on Neusilin FH2. To identify the dominant release mechanism, the data from the in vitro release investigation was fitted into the various mathematical release models. The results are shown in Table 5.

### 3.10 Differential scanning calorimetry (DSC) on solid LSES

The amorphous Neusilin $FH_2$ powder (Figs. 6, 7) had a broad endothermic melting peak at 230.9 °C, whereas the more crystalline ART and LUM powders had sharp endothermic melting peaks at 89.7 °C and 134.7 °C, respectively.

### 3.11 Antimalaria studies

ART-LUM LSES, solid ART-LUM, and commercial ART-LUM tablet brands had antimalarial activities (AA) of 85.21%, 72.63%, and 55.03%, respectively (Table 6). Furthermore, the AA of the aqueous dispersion of ART-LUM was 21.2%. The ART-LUM LSES, which demonstrated the highest antimalarial activity, had the least % parasitemia (5.0 ± 1.83). Every patient's clinical sign of treatment effectiveness is a decrease in parasitemia. The hematological parameters (PCV, RBC count) were found to be significantly higher ($P < 0.05$) in all drug-treated animals compared to placebo treated animals (Table 7).

### 3.12 Preliminary anti-inflammatory studies

The sheep red blood cell (SRBC)-injected mice exhibited a remarkable increase in delayed-type hypersensitivity reaction (0.80 ± 0.06) and haemagglutination antibody titre (96 ± 18.47) indicating stimulation of cellular and humoral immunity, respectively (group 1). However, the administration of ART-LUM LSES elicited significantly lower ($p < 0.05$) haemagglutination antibody (HA) titre and delayed type hypersensitivity (DTH) in the mice compared to the untreated group (group 1). The differential counts of white blood cells did not vary much across all treated groups. The groups that received either aqueous dispersion of pure ART or ART LSES (groups 5, 8) showed lower values of HA and DTH compared to the groups that received aqueous dispersion of pure LUM, LUM LSES (groups 6, 9), aqueous dispersion of pure ART-LUM or ART-LUM LSES (group 4, 7). Groups that received LSES (groups 7, 8, and 9) recorded lower values of HA and DTH than the groups that received the commercial drug (group 3). Refer to Tables 8 and 9.

### 3.13 Histopathology studies

Histopathology studies were carried out to investigate the safety of the LSES in organs. The effects of the formulations at low doses (2 mg/kg artemether and 12 mg/kg lumefantrine), medium doses (4 mg/kg artemether and 24 mg/kg lumefantrine) and high doses (8 mg/kg artemether and 48 mg/kg lumefantrine) on the liver,

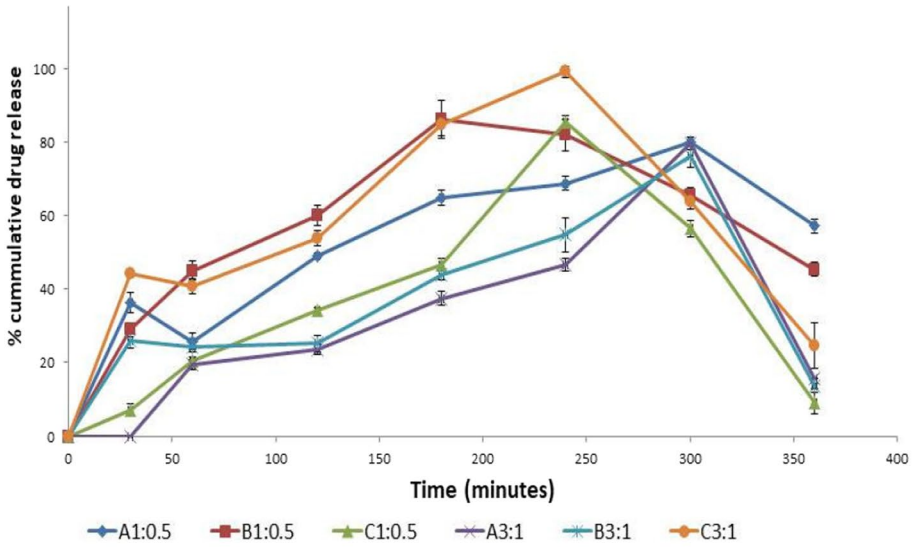


a: Release profile of artemether- loaded LSES in SGF pH 1.2 (Dialysis membrane technique)

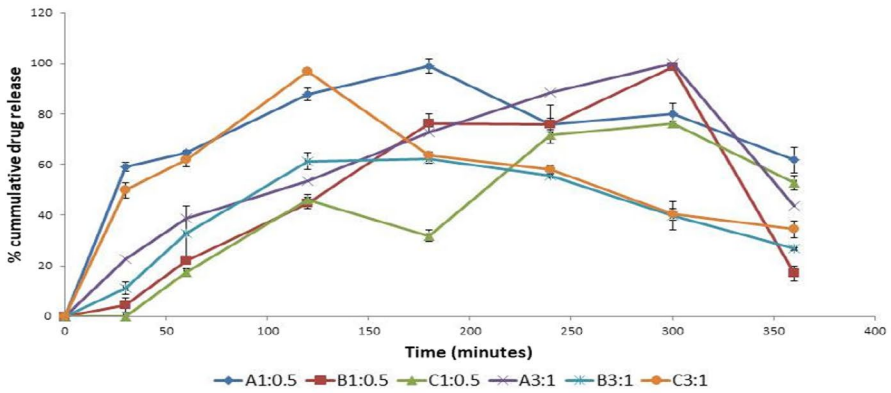


b: Release profile of artemether-loaded LSES in phosphate buffer pH 6.8 (Dialysis membrane technique)

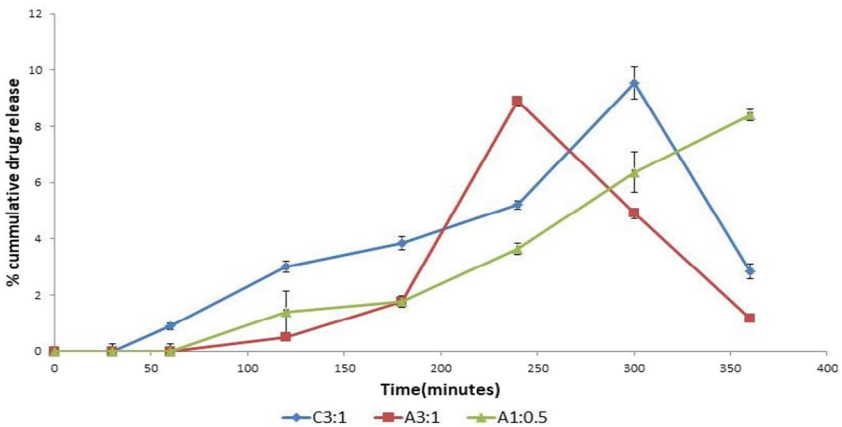


c: Release profile of lumefantrine -loaded LSES in phosphate buffer pH 6.8 (Dialysis membrane technique

**Fig. 5 a–f** Release profile of artemether and lumefantrine loaded LSES in SGF pH 1.2 and Phosphate buffer pH 6.8. Each value designates mean ± S.D of $n = 3$

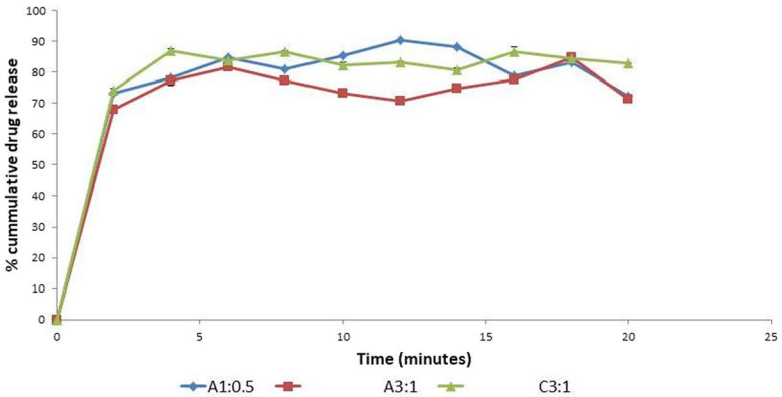


d: Release profile of lumefantrine -loaded LSES in phosphate buffer pH 6.8 (rotating basket method)

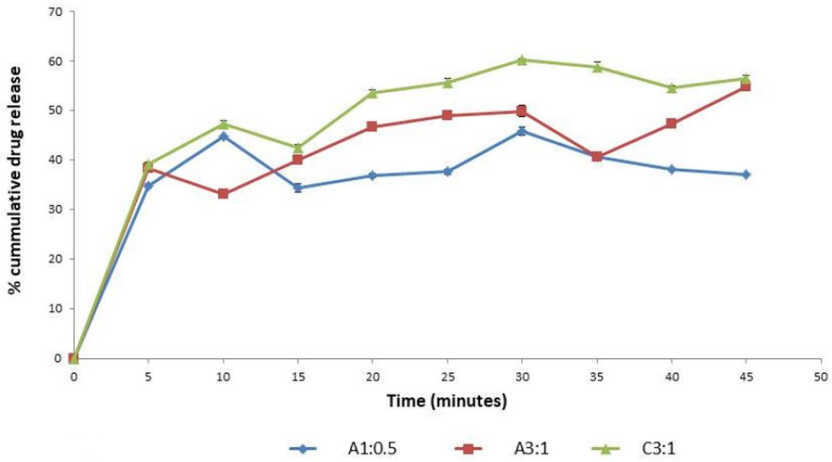


e: Release profile of Neusilin FH2-based lumefantrine LSES in SGF pH 1.2 (rotating basket method)

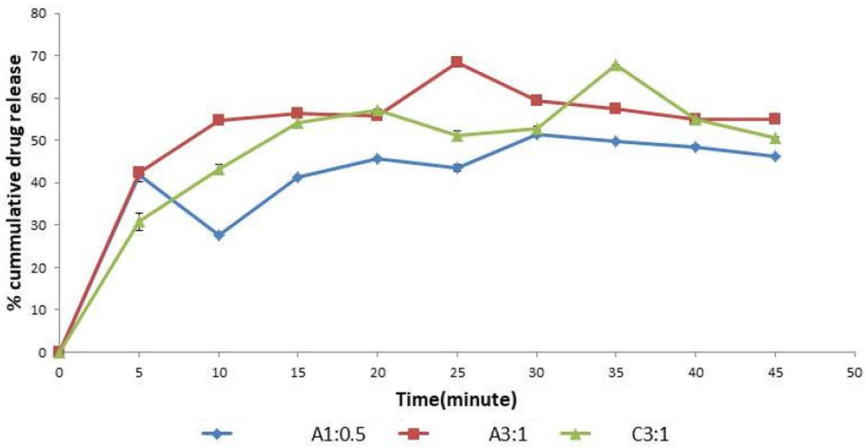


f: Release profile of Neusilin FH2-based lumefantrine LSES in phosphate buffer pH 6.8 (rotating basket method)

**Fig. 5** continued

**Table 5** Release kinetics studies

| Batches | Dissolution technique/media | Zero order $R^2$ | First order $R^2$ | Higuchi $R^2$ | Krosmeyers Peppas $R^2$ | Krosmeyers Peppas $n$ |
|---|---|---|---|---|---|---|
| C 3:1 | Rotating basket (SGF pH 1.2) | 0.387 | 0.671 | 0.876 | 0.975 | 0.239 |
| C 3:1 | Rotating basket (phosphate buffer pH 6.8) | 0.437 | 0.738 | 0.890 | 0.944 | 0.312 |
| A 1:0.5 | Dialysis membrane (SGF pH 1.2) | 0.742 | 0.899 | 0.948 | 0.949 | 0.479 |
| C 1:0.5 | Dialysis membrane (SGF pH 1.2) | 0.955 | 0.886 | 0.789 | 0.949 | 0.479 |
| B 1: 0.5 | Dialysis membrane (phosphate buffer pH 6.8) | 0.965 | 0.886 | 0.789 | 0.949 | 0.479 |
| A 3: 1 | Dialysis membrane (phosphate buffer pH 6.8) | 0.917 | 0.977 | 0.981 | 0.949 | 0.479 |

kidney, and spleen were investigated after oral administration to the mice. Microscopic examination of the liver sections of the uninfected and untreated control groups showed apparently normal plates of hepatocytes radiating away from the central vein and portal areas comprising the hepatic artery, hepatic portal vein, and bile ducts. On the other hand, the post-infection untreated group had severe periportal mononuclear cellular infiltration (inflammation), widespread hemosiderosis (evidence of red cell haemolysis and erythrophagocytosis), and hepatocyte necrosis. The kidney sections from the uninfected and untreated control groups had normal histological architecture, comprising the glomerulus and renal tubules within the interstitial tissues. However, the post-infection untreated group had prominent mononuclear cellular infiltration of both the glomerulus and renal tubules (glomerulonephritis). These were mildly seen in the low and medium dose groups, but the high dose group had tubular vacuolation (nephrosis). The spleen sections showed varying degrees of haemosiderosis (evidence of red blood cell breakdown), megakaryocyte proliferation (evidence of hemopoiesis), and a reduction in lymphoid tissue (lymphoid hypoplasia) (Table 10). The infected untreated group showed severe liver damage. Various degrees of improved histopathological changes were seen in the liver, kidney, and spleen of all the treated groups when compared to the post-infection untreated group. Effectiveness and safety appear to be associated with low or medium dose LSES; however, high dose administration of the formulations was associated with moderate hepatic necrosis and tubular degeneration/nephrosis (Figs. 8, 9, 10). Therefore, it is important to stay within the recommended dose of artemether and lumefantrine during malaria treatment to avoid the damage caused to the liver and kidney at high doses.

## 4 Discussion

Natural fats/lipids were utilized as part of the excipients; therefore activated charcoal and bentonite were used for purification process. Activated charcoal and bentonite, have been previously used for lipid purification [15]. They have the ability to adsorb impurities and thus produce purified oil or lipids.

Lumefantrine had remarkable solubility in oleic acid. The high solubility of lumefantrine may be attributed to the ionic hydrophobic interaction between the tertiary amine of LUM and the carboxylic group of oleic acid [20]. Therefore oleic acid was selected as the oil phase for the lumefantrine formulations. On the other hand, ART had the highest solubility in palm kernel, hence its choice as an oil phase. Drug solubility in oil is very crucial as it forms the core for the dissolved drug and facilitates self-emulsification of the lipophilic drug [9, 36].

The post-formulation visual test/refrigeration/centrifugation tests were to typically predict stability, the prospective effect of transportation, mechanical impacts, and environmental conditions on the LSES. A kinetically/thermodynamically unstable LSES would be tractable to drug crystallisation under minimal centrifugal force which may portend amenability to precipitation in aqueous phase.

The ART LSES did not indicate any form of precipitation in aqueous acid or phosphate buffer in the aqueous dilution test; it is suggestive of kinetic stability. Unless an overwhelming external influence impinges on a thermodynamically stable LSES, it will not undergo phase separation, Ostwald ripening, or drug crystallisation. Mechanistically speaking, kinetic stability implies that between the reactant state (LSES) and the product state (phase separated emulsion) there exists a high reaction barrier but the free energy remains negative ($\Delta G < 0$). In thermodynamic stability, from the reactant to the product state the free energy is greater than zero ($\Delta G > 0$); implying that reaction will not take place unless external energy is introduced [37]. The presence of Kolliphor EL (with critical micelle concentration, (CMC) of 0.02%) and Kollidon VA 64 fine in LUM LSES imparted kinetic stability since phase separation and drug crystallisation were not observed.

The observed emulsification time values of Kolliphor HS 15 LUM LSES and some of the Kolliphor EL-based formulations containing Kollidon VA 64 were within

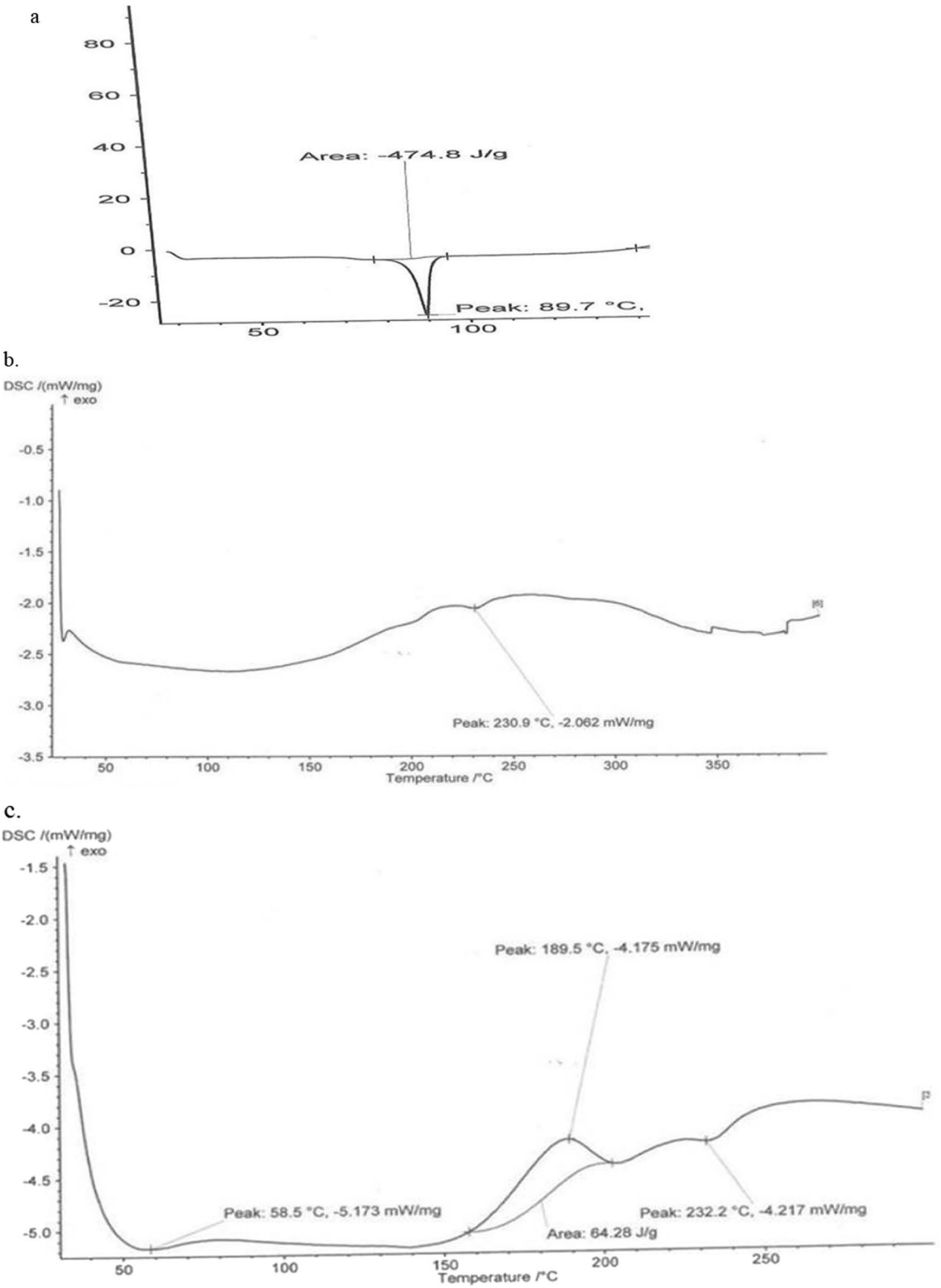


**Fig. 6** DSC thermograph of **a** artemether pure drug, **b** neusilin and **c** artemether loaded solid LSES

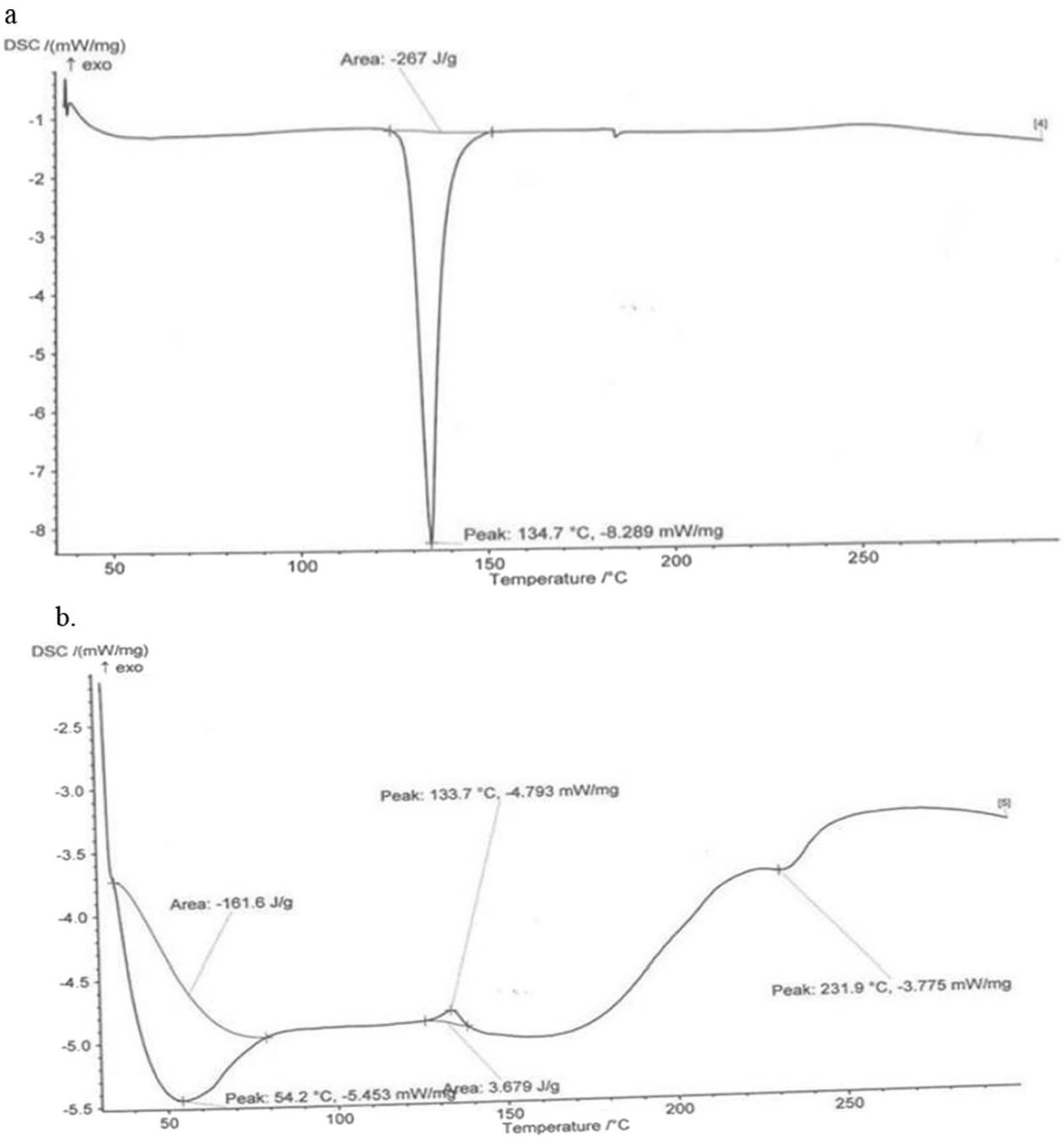


**Fig. 7** DSC thermograph of **a** Lumefantrine pure sample and **b** Lumefantrine loaded solid LSES

the acceptable range of 0–1 min as previously reported [7]. Phosphate buffer solution served as the emulsifying medium for Kolliphor HS 15 LUM LSES because LUM had crystallized out in SGF pH 1.2. Drug crystallisation in this aqueous acid may be attributed to the weakening of the bond between the amine group of lumefantrine and the carboxylic group of oleic acid by hydrogen ions from HCl [20]. To correct this physicochemical deficit, Kolliphor EL-based LUM LSES was formulated to promote stability in aqueous acid. Kolliphor EL has been reported to most efficiently emulsify oleic acid as it has three fatty acid chains attached to the PEG glycerol [20, 38, 39]. While Kolliphor EL successfully ensured non-LUM recrystallisation in aqueous acid, Kollidon VA 64 scaled down ET and reinforced crystallisation inhibition. As a result, the addition of Kollidon VA 64 to the

**Table 6** Percentage antimalarial activities across the groups

| Groups | Antimalarial activity (%) |
|---|---|
| Group A | 56.36 |
| Group B | 43.05 |
| Group C | 72.63 |
| Group D | 77.07 |
| Group E | 84.23 |
| Group F | 85.21 |
| Group G | 55.03 |
| Group H | – |
| Group I | – |
| Group J | – |
| Group K | 15.18 |
| Group L | 20.12 |
| Group M | – |
| Group N | – |
| Group P | 21.20 |

**Table 7** Hematological parameters of the animals after infection and after treatment

| Groups | After infection | | After treatment | |
|---|---|---|---|---|
| | PCV (%) | RBC ($10^6$) | PCV (%) | RBC ($10^6$) |
| Group A | 31.8 ± 1.79 | 8.44 ± 0.52 | 41 ± 1.15 | 10.54 ± 0.31 |
| Group B | 30.4 ± 2.07 | 8.51 ± 0.51 | 41 ± 1.83 | 9.90 ± 0.42 |
| Group C | 27 ± 11.90 | 7.97 ± 0.76 | 42 ± 2.90 | 10.50 ± 0.12 |
| Group D | 31.17 ± 3.60 | 7.87 ± 0.77 | 40.5 ± 3.11 | 10.39 ± 0.70 |
| Group E | 32 ± 3.65 | 8.51 ± 0.13 | 36.67 ± 3.21 | 10.49 ± 0.17 |
| Group F | 35.4 ± 3.71 | 7.08 ± 0.51 | 42.75 ± 2.22 | 10.36 ± 0.64 |
| Group G | 21.4 ± 1.95 | 5.05 ± 0.42 | 34.4 ± 2.30 | 9.32 ± 0.41 |
| Group H | 32.25 ± 3.30 | 6.60 ± 0.68 | 33.25 ± 2.75 | 8.76 ± 0.43 |
| Group I | 30.67 ± 2.50 | 7.75 ± 0.96 | 31.2 ± 1.92 | 7.75 ± 0.53 |
| Group J | 32.17 ± 2.71 | 6.76 ± 0.72 | 31.2 ± 1.30 | 7.5 ± 0.85 |
| Group K | 30.20 ± 1.48 | 6.87 ± 0.50 | 28.67 ± 3.05 | 7.70 ± 0.74 |
| Group L | 31.4 ± 1.67 | 7.10 ± 0.68 | 31.67 ± 1.53 | 7.44 ± 0.12 |
| Group M | 24 ± 2.97 | 6.12 ± 0.49 | 35.6 ± 3.65 | 8.41 ± 1.25 |
| Group N | 23.2 ± 3.03 | 5.67 ± 0.42 | 34.75 ± 3.59 | 6.61 ± 0.53 |
| Group O | 49.5 ± 3.70 | 10.72 ± 0.14 | 48.25 ± 3.10 | 10.69 ± 0.24 |
| Group P | 23.2 ± 3.83 | 5.93 ± 0.50 | 33.6 ± 3.58 | 8.43 ± 0.29 |

LUM LSES improved stability and may have prevented drug crystallisation during GIT transit. Essentially, LSES are mostly preferred to emulsify in a short time to arguably promote a short onset of action, consistent absorption, and bioavailability. Whereas Kolliphor EL apparently promoted kinetic stability in aqueous acid, Kollidon VA 64 fine did reinforce it by probably sustaining the inhibition of nucleation, creaming, and phase separation. In this way molecularly dissolved LUM maintained its entrapment in the droplet, and thus mitigated LUM recrystallisation via the "parachute effect which is characterized by non-crystallisation of solubilized poorly soluble drug from dosage form immersed in aqueous phase" [40–42]. Kollidon VA 64 fine is known to prevent the "spring effect," which involves the diffusion of solubilized poorly soluble drugs from dosage forms to crystallize out in the surrounding aqueous GIT environment [40].

**Table 8** Effects of Artemether and Lumefantrine loaded LSES on SRBC induced delayed-type hypersensitivity and haemagglutination titre in mice

| Treatment groups | HA | DTH response (mm) |
|---|---|---|
| Group 1 | 96 ± 18.47 | 0.80 ± 0.06 |
| Group 2 | 6 ± 1.15 | 0.15 ± 0.03 |
| Group 3 | 50 ± 26.61 | 0.70 ± 0.22 |
| Group 4 | 32 ± 11.31 | 0.40 ± 0.11 |
| Group 5 | 20 ± 6.93 | 0.35 ± 0.06 |
| Group 6 | 26 ± 6.00 | 0.38 ± 0.06 |
| Group 7 | 42 ± 13.61 | 0.43 ± 0.11 |
| Group 8 | 34 ± 11.49 | 0.40 ± 0.08 |
| Group 9 | 44 ± 28.56 | 0.50 ± 0.14 |

Kollidon VA 64 fine caused a sudden drop in particle size—403 nm and 505 nm, as Kolliphor EL concentration increased to 60% and 65%, respectively. This was lower than the particle size seen in Kolliphor HS 15 (1579–2022 nm). Kolliphor HS 15 LSES, may have been assaulted by Laplace pressure in an aqueous acid medium. Laplace pressure is the resultant outcome of interfacial tension existing at the curved interface of droplets dispersed in another liquid. During emulsification, Laplace pressure could cause an emulsion to become thermodynamically unstable by collapsing smaller droplets and their contents into larger ones due to higher pressure impingement on the inner concave interface than on the convex interface of the droplets. In the process of smaller droplets merging with larger ones, drug crystallisation ensues. This Ostwald ripening process, accelerated by the ionic strength of HCl, may have contributed to the rapid precipitation of LUM from Kolliphor HS 15 LSES droplets in pH 1.2 medium. The surfactant (Kolliphor HS 15) has a critical micelle concentration, (CMC) of 0.002–0.05%. Increased surfactant concentration probably attenuated Laplace pressure and Ostwald ripening through further interfacial tension reduction. ART LSES showed particle sizes ranging from 8.95 to 39.88 nm and PDI of 0.09–0.25. ART LSES fulfilled all optimal conditions (nanodroplet size, PD) for a typical kinetically

**Table 9** Effects of Artemether and Lumefantrine loaded LSES on white blood cell differentials

| Groups | White blood cell differentials (mean ± SD) | | | |
|---|---|---|---|---|
| | Lymphocytes (%) | Neutrophils (%) | Monocytes (%) | Eosinoph (%) |
| Group 1 | 70.75 ± 4.82 | 23.00 ± 4.20 | 5.50 ± 0.96 | 1.00 ± 0.41 |
| Group 2 | 75.00 ± 4.65 | 21.50 ± 4.79 | 3.00 ± 0.00 | 0.50 ± 0.50 |
| Group 3 | 73.75 ± 1.31 | 22.25 ± 2.46 | 2.75 ± 0.85 | 0.75 ± 0.48 |
| Group 4 | 73.25 ± 4.94 | 19.75 ± 3.97 | 4.25 ± 1.03 | 2.75 ± 0.85 |
| Group 5 | 66.50 ± 5.25 | 29.00 ± 5.69 | 3.50 ± 0.95 | 1.50 ± 0.95 |
| Group 6 | 67.00 ± 6.61 | 32.00 ± 5.94 | 5.50 ± 0.50 | 2.00 ± 0.82 |
| Group 7 | 68.00 ± 6.94 | 26.50 ± 6.02 | 4.25 ± 1.18 | 1.25 ± 0.75 |
| Group 8 | 67.25 ± 3.54 | 24.75 ± 2.56 | 5.50 ± 0.87 | 2.50 ± 1.26 |
| Group 9 | 69.50 ± 3.20 | 20.50 ± 0.96 | 6.50 ± 0.96 | 3.00 ± 1.29 |

Results are expressed in Means ± SD (n = 5)

Group 1—SRBC + distilled water; Group 2—SRBC + diluent only; Group 3—SRBC + commercial drug sample (40 mg/kg); Group 4—SRBC + Artemether + Lumefantrin solution (40 mg/kg); Group 5—SRBC + Artemether solution (40 mg/kg); Group 6—SRBC + Lumefantrin solution (40 mg/kg); Group 7—SRBC + Artemether + Lumefantrin formulation (40 mg/kg); Group 8—SRBC + Artemether formulation (40 mg/kg); Group 9—SRBC + Lumefantrin formulation (40 mg/kg)

**Table 10** Summary of histopathological effects as seen in the liver, kidney and spleen

| Lesion | Control (normal saline) | 2 mg/kg ART + 12 mg/kg LUM | 4 mg/kg ART + 24 mg/kg LUM | 8 mg/kg ART + 48 mg/kg LUM | Infected untreated |
|---|---|---|---|---|---|
| Haemosiderosis (liver) | 0,0,1 | 3,1,2 | 2,2,1 | 2,1,1 | 3,2,3 |
| Periportal mononuclear cells infiltration (liver) | 0,0,0 | 2,2,1 | 1,1,2 | 0,0,1 | 3,3,3 |
| Hepatic necrosis/vacuolations (liver) | 0,0,0 | 1,0,2 | 1,1,1 | 3,2,2 | 2,1,1 |
| Kupffer cell hyperplasia (liver) | 0,0,0 | 1,1,2 | 1,0,1 | 0,0,1 | 3,3,2 |
| Mononuclear inflammatory cells infiltration (kidney) | 0,0,0 | 1,1,2 | 1,0,2 | 0,0,1 | 3,2,2 |
| Tubular degeneration/vacuolations/nephrosis (kidney) | 0,0,0 | 1,0,1 | 1,1,1 | 3,2,2 | 2,1,1 |
| Haemosiderosis (spleen) | 0,0,1 | 3,1,1 | 2,1,1 | 2,1,0 | 3,2,1 |
| Megakaryoblast hyperplasia (spleen) | 0,0,1 | 3,1,2 | 2,2,1 | 2,1,1 | 3,2,3 |
| Lymphoid hypoplasia (spleen) | 0,0,0 | 1,1,2 | 1,0,2 | 1,0,1 | 3,2,2 |
| Macrophages/splenic phargocytosis (spleen) | 0,0,1 | 3,1,1 | 2,1,1 | 2,1,0 | 3,2,1 |

*LUM* lumefantrine, *ART* artemether, normal (0), mild (1), moderate (2), and severe (3)

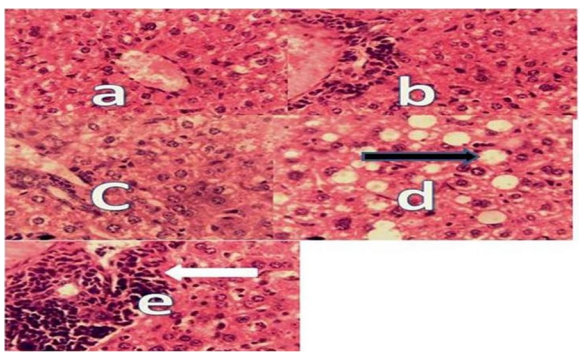


**Fig. 8** Photomicrograph of the liver sections from group **a**–**e** X400. Note the periportal mononuclear cellular infiltration, inflammation in group **e** (white arrows) and hepatocyte vacuolations in group **d** (black arrows) × 400

and probably thermodynamically stable microemulsion [43]. Although most of the LUM LSES particle sizes were within the small micrometre or large nano-range, the observed stability of LUM LSES during aqueous dilution and dissolution studies may sustain drug-dissolved droplets until they transit to the intestinal milieu. Within the intestine, further emulsification of the droplets by a mixture of endogenous bile salts and phospholipids would ensure consistent absorption [44–46]. Thus, with the exception of droplets that are susceptible to lymphatic uptake, both micro-scale and nano-scale droplets are liable to lipase hydrolysis in the intestine. Hence, we posit that as far as Kolliphor EL-Kollidon VA 64 LSES is concerned, once its kinetic

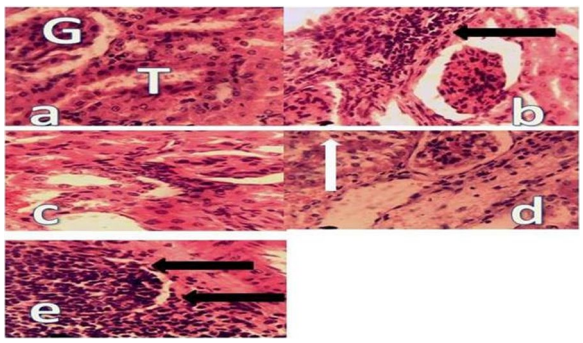


**Fig. 9** Photomicrograph of the kidney section from group **a**–**e**. Note the normal architecture comprising the glomerulus (G) and renal tubules (T) within the interstitial tissues in group a and mononuclear cellular infiltration of both the glomerulus and the renal tubules (glomerulonephritis) in the infected untreated group **e** (black arrows) which were midly seen in the low dose group **b** (black arrows) but not in the medium and high dose group **c**, **d**. See tubular nephrosis or vacuolation in group **c** (white arrow) ×400

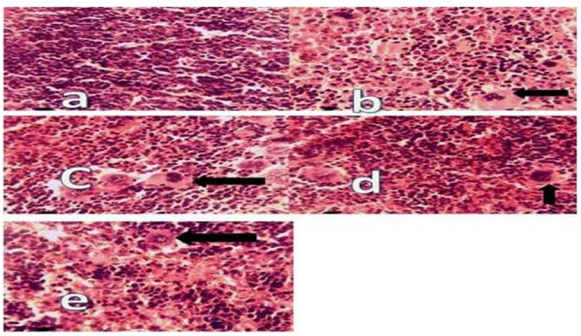


**Fig. 10** Photomicrograph of the spleen section from group **a**–**e**. *Note* megakaryocyte proliferation (evidence of hemopoiesis)—black arrows and reduction in lymphoid tissue (lymphoid hypoplasia) in all except the un-infected untreated control group **a** ×400. Group a treated with normal saline (control), group **b** low dose, group **c** medium dose, group **d** high dose and group **e** infected untreated

stability properties ensure intact droplets in the stomach and intestine for 2–3 h (gastric emptying time), droplet size may be of little consequence. The critical question worthy of consideration in the treatment of malaria with ART and LUM is whether the drugs will remain solubilized in GIT fluid without crystallisation prior to absorption. Due to their poor solubility in aqueous and aqueous acid phases, most formulation attempts to improve the solubility of ART and LUM require nutritional aids (e.g. milk) to improve bioavailability or surfactants in the dissolution medium to preclude crystallisation. However, our present Kolliphor EL-Kollidon VA 64 LUM LSES formulations are potentially capable of preventing drug crystallisation, improving absorption, enhancing bioavailability and mitigating resistance caused by sub-lethal drug concentration [10, 47, 48].

The granulation properties generally indicate fair or passable flow behaviour. The angle of repose is a measure of the internal friction or cohesion of the particles. It is high if cohesive and other forces are high and vice versa. Generally, if the angle exceeds 50°, the powder will not flow satisfactorily while materials having values near the minimum, circa 25°, flow easily and well [26, 49]. It should be noted that the liquid LSES was adsorbed onto Neusilin without the addition of flow aid. Based on the angle of repose, Hausner's quotient, and Carr's compressibility index results, batches $B_{3:1}$ (ART LSES) and $A_{3:1}$ (LUM LSES) demonstrated acceptable granulation properties. It has been reported that HQ values of less than 1.25 indicate good flow, while values greater than 1.25 indicate poor flow. HQ values between 1.25 and 1.5 require the addition of a glidant to improve flow [27]. The flow scale of powder and granulations has been described as excellent, for values of CI within 5–15%, good for 12–16% and fair to passable for 18–21%, while between 23 and 35% are said to be poor, 33–38% are very poor and values > 40% are extremely poor [27]. HQ and CI are useful indices for assessing drug powder and granule flow properties. These flow indices are not individually sufficient to confirm powder or granulation flowability. For instance, a powder could have a high Carr's compressibility index and still flow well under gravity and vice versa. Therefore, it has been reported that no one test or index could reliably reflect powder flow ability. Furthermore, we observed that unusual consolidation of the granules occurred in the tapped density experiments. This could be attributed to the weak bond formation between the granules or the probable low tensile strength of the granules formed. Wet granulation is often associated with the formation of liquid bridges between particles, with the tensile strength of these bonds increasing as the quantity of granulating fluid increases. Thus, in the process of drying, the formation of interparticulate bonds due to the fusion or recrystallisation and curing of the binding agent takes place [50–52]. In this study, the wetting agent used was ethanol, without any binding agent. Therefore, the particles of the granules formed were interbonded weakly, which explains the amount of deformation that ensued upon tapping, as is evident in the high tapped density values. So far, the general flow behaviour of the granulations is sufficient to guarantee free and easy flow into hard gelatin capsules.

The DSC spectra showed the sustained solvation form of the drugs within the Neusilin FH2 matrix resulted in the broad melting peaks of solid ART and LUM LSES at 58.5 °C and 54.2 °C, respectively [51, 53]. By implication, the solid carrier advantageously amorphized the two drugs and showed no potential excipient incompatibility.

The high drug loading efficiency was an indication of the high drug entrapment capacity of the LSES. Achievement of high drug entrapment is more predictable with LSES than with polymeric nanoparticles. The incorporation of a liquid self-emulsifying formulation into a solid dosage form may combine the advantages of LSES with those of a solid dosage form and overcome the disadvantages (including leakage from the capsule shell) associated with encapsulating liquid formulations.

The Kolliphor EL LUM LSES showed an initial burst release of over 80% of drug within 3–4 min in SGF pH 1.2 and phosphate buffer pH 6.8 (graph not shown) while the Neusilin FH2-based LUM LSES had a maximum release of about 60% in SGF pH 1.2 and 51.54–67.81% in phosphate buffer solution pH 6.8. Recall that the change of surfactant from Kolliphor HS 15 to Kolliphor EL with the inclusion of Kollidon—VA 64 prevented crystallisation of LUM in the aqueous acid media. Consequently, the release study further confirmed that no external dissolution aids was required in the dissolution studies. The observed erratic release of LUM from the solid LSES may be attributed to the varying desorption times of LSES from the adhered insoluble particle surfaces (Neusilin $FH_2$). On the other hand, the diminished release of LUM could be attributed to stronger adherence to and entrapment of LUM within the three-dimensional structure of Neusilin. Previous workers have reported similar observations [54–57]. The successful inhibition of LUM crystallisation in aqueous acid by Neusilin $FH_2$ may be due to the impartation of a micro-alkaline environment that probably increased the aqueous acid pH to an alkaline scale. At a 5% w/v slurry concentration, Neusilin $FH_2$ records a pH of 9.7 [58]. Recall that at pH of 7.2, the Kolliphor HS 15 LSES was not susceptible to LUM crystallisation. Thus, at an elevated pH of 9.7, a sufficient alkaline milieu fostered emulsion stability.

The $R^2$ value seen in the kinetic studies reveals the degree to which the formulations suit the mathematical models. In terms of how well each batch fit, the Korsmeyer–Peppas model performed better than the Higuchi model for all formulations. Unlike the Higuchi release model, which explains that the release of drugs from an insoluble matrix is dependent on the square root of time and based on fickian diffusion, the Korsmeyer–Peppas model describes a system where the fractional release of drugs is exponentially related to time [59]. The Korsmeyer kinetic model is often used when the release mechanism is not evident or when there are numerous release occurrences. The release mechanism is defined by the "*n*" value of the Korsmeyer–Peppas model. The "*n*" value between 0 and 0.5 supports fickian diffusion, however n between 0.5 and 1 indicates mass transfer or anomalous transport [60]. All of the formulations' "*n*" values were lower than 0.5 depicting fickian diffusion (Table 5).

The antimalarial study reinforces the superiority of combination therapy over monotherapy. This is not surprising since the two drugs are known to cause hemolysis of red blood cells together with parasite clearance. The incomplete drug desorption from Neusilin $FH_2$ may have been responsible for the reduction in antimalarial activity recorded by solid LSES in comparison with liquid LSES. The gastroprotective role of LSES droplets on ART and general solubilisation of LUM and ART probably enhanced absorption, bioavailability, and antimalarial activity [4, 48, 61]. The alkaline pH of Neusilin $FH_2$ may have also offered gastro protection to ART by increasing the pH of the micro-environmental pH. Expectedly, the self-emulsified droplets, aided by their high surface area-to-volume ratio, may have promoted consistent drug absorption across intestinal epithelium or via the lymphatic route. Lymphatic transport could be occasioned by highly lipophilic drugs, long-chain fatty acids, and LSES via association with lipoproteins [62]. On the other hand, the non-enhancement of the solubilities of artemether and lumefantrine by commercial tablet brands may have resulted in poor/erratic absorption and poor bioavailability. In an industrial setting, the formulation pharmacist and company policy makers could choose between the option of liquid LSES or solid LSES given their kinetic stability (especially absence of drug crystallisation) and high antimalarial activity prospects. Whereas the solid LSES has shorter tabletability steps, the liquid LSES enjoys faster emulsification time. If capsule leakage is a potential disadvantage to tackle in liquid LSES, possible delayed drug (LUM) desorption may be a demerit to unravel in solid LSES.

Inflammations develop by changing the response of T-cells, thereby causing irregularities in the immune system, which are associated with the migration of leukocytes, especially neutrophils. The effect of artemether-lumefantrine LSES on the immune system was demonstrated using the HA and DTH tests. The DTH reaction is a type-IV hypersensitive immune response that provides a functional in vivo assessment of cell-mediated immunity in animals [32]. Generally, the T-helper 1 (Th1) cell-mediated immune response oversees the elimination of intracellular parasites while the T-helper 2 cell-mediated immune response is responsible for the elimination of extracellular parasites

[63]. Activation of the Th1 cells prompts the release of cytokines that initiate the activation and accumulation of macrophages, enhancement of vascular permeability, induction of vasodilation, and consequently inflammation [64]. This process was responsible for the swelling of the foot pad observed in the mice. The present study has revealed that ART and LUM LSES have good anti-inflammatory effects with immune system modulation as the possible mechanism of action. The lipid vehicle, which improved solubility, consequently improved the drug's anti-inflammatory activities compared to the commercial brand. Surprisingly, from the results obtained, the LSES vehicle (without the drugs) elicited a remarkable decrease in HA and DTH. The fatty acid composition, especially oleic acid, has been known to play important roles in immune and inflammatory responses. Previous studies have reported the role of oleic acid in suppressing lymphocyte proliferation and inhibiting cytokines [65]. These fatty acids have also been reported to be useful in speedy wound healing [66]. Recall that the bond between the carboxylic group of oleic acid and the amine group of the lumefantrine may have affected the availability of free oleic acid. The white blood differential counts did not vary much across all treated groups (Table 9). This suggests that the white blood differential count may not be a perfect index to measure anti-inflammatory activity and, hence, there is a need to evaluate possible markers expressed on the surface of the white blood cells for a more accurate interpretation. ART had more immunomodulatory and anti-inflammatory effects than LUM. This is consistent with previous studies where artemether inhibited neuroinflammation-mediated HT22 neuronal toxicity in liposaccharide (LPS)-stimulated BV2 microglia/HT22 neuron co-culture after 24 h [16]. This suggests that artemether LSES and, to a lesser extent, lumefantrine LSES abate the production of cytokines that trigger Th1-mediated inflammatory immune responses. This activity may be found useful in the treatment of inflammations associated with diseases like COVID-19, which is known to induce Th1-hyperinflammatory immune responses in human lungs and a systemic inflammatory cascade [67]. Studies have shown that SARS-CoV 2 infection triggers increased production of interleukin-2 (IL-2), IL-6, IL-7, granulocyte-colony stimulating factor, macrophage inflammatory protein 1, monocyte chemoattractant protein 1, interferon-inducible protein 10, tumour necrosis factor (TNF-), and ferritin, leading to fatal hypercytokinemia with failure of the lungs and death [68]. It has been reported that COVID-19 African patients with long exposure to malaria had lower levels of inflammatory cytokines and mortality [19]. However, the antimalarial drugs used in treating malaria during the exposure period were not countenanced to also cause blunting of inflammatory cytokines. Therefore, further studies evaluating the long-term exposure effect of antimalarials (ART-LUM) on inflammatory cytokines ought to be conducted to confirm if malaria or drug exposure or both should be given credit for the blunting effect. Until then, it suffices that our present finding has confirmed ART-LUM to exert a blunting effect on some inflammatory markers and may hold promise in mitigating cytokine storm possibilities during COVID-19 infection.

The histopathology result of the liver sections is attributed to the erythrocytic stage of the parasitic life cycle. In response to the damage, the kupffer cells actively proliferate, break down ruptured red blood cells and split haemoglobin molecules, thus leading to haemosiderosis (linked with anaemia) and eventually hepatic necrosis. The high-dose treated groups were devoid of the lesions seen in the untreated group but had benign hepatocyte vacuolations [69]. The low and medium dose groups had milder presentations of periportal mononuclear cellular infiltration, hemosiderosis, and hepatocyte necrosis. The liver damage seen with the infected untreated group may be attributed to the erythrocytic stages of the plasmodium life cycle and toxins produced by the parasite. This may have resulted in the active proliferation of the kupffer cells (Kupffer cell hyperplasia), thereby breaking down ruptured red blood cells by phagocytic action and splitting the haemoglobin molecules. The resultant pathological effect is the accumulation of iron in the liver (haemosiderosis), which is often linked to anaemia and could extend to the rapid death of the parenchymal cells of the liver (hepatic necrosis) that is evident with untreated malaria [70].

## 5 Conclusion

Nanosized artemethers (8–39 nm) and micro-scale LUM (1579–2022 nm) lipid self-emulsifying systems (LSES) with improved stability and rapid emulsification time (about 1 min) were produced and investigated. The solidification of liquid LUM LSES with Neusilin $FH_2$ or reformulation of LSES with Kolliphor EL and Kollidon VA 64 fine improved the stability and prevented the crystallisation of the micro-scale LUM LSES in aqueous acid. Hence, there was no need for the inclusion of dissolution aides in the pH 1.2 dissolution medium. The increased antimalarial activities (85.21%) and (72.63%) of the liquid and solid LSES, respectively, could be attributed to improved drug solubilisation by the LSES in contrast with the commercial drug (55.03%). ART and LUM LSES exerted palpable anti-inflammatory effects. Modulation of the immune system could be a possible explanation for the observed anti-inflammatory effects. The artemether and lumefantrine LSES demonstrated a good safety profile as seen in

the histopathological studies; however, moderate hepatic necrosis and tubular degeneration/nephrosis were associated with high dose administration of the formulations. The use of ART and LUM LSES may be a useful management strategy for COVID-19 induced inflammations in patients with malaria. It is safe to conclude that for the first time we have prepared a LUM micro-scale lipid system with improved solubility / enabled stability in aqueous acid and a stable ART nano-scale lipid system (with improved stability) from palm kernel oil.

**Abbreviations**

| | |
|---|---|
| LSES | Lipid self-emulsifying system |
| ART | Artemether |
| LUM | Lumefantrine |
| PKO | Palm kernel oil |
| ET | Emulsification time |
| OA | Oleic acid |
| SNEDDS | Self-nano-emulsifying drug delivery system |
| GIT | Gastro intestinal tract |
| DS | Droplet size |
| PDI | Polydispersity index |
| GRAS | Generally regarded as safe |
| SRBC | Sheep red blood cells |
| HA | Haemagglutination antibody titre |
| DTH | Delayed type hypersensitivity |
| HQ | Hausner's quotient |
| CI | Carr's compressibility index |
| AA | Antimalarial activities |
| DSC | Differential scanning calorimetry |
| LPS | Liposaccharide |
| TNF | Tumour necrosis factor |
| IL-2 | Interleukin-2 |
| IL-6 | Interlukin-6 |
| IL-7 | Interlukin-7 |

**Acknowledgements**
We are grateful to Dr. Onoja of the department of veterinary parasitology who helped with the histopathology studies and Prof Moji Adeyeye who did the droplet size analysis of the formulations. We also appreciate Fuji (Japan), BASF and Gateffose (Germany) for the materials supplied.

**Author contributions**
O.L.U.: Performed the experiment; Analysed and interpreted data; Contributed reagents, materials, analysis tools or data; Wrote the paper. I.V.O.: Conceived and designed the experiment; Analyzed and interpreted data; supervised the work. J.N.O.: Performed the experiment; Analysed and interpreted data. C.M A.: Contributed reagents, materials, analysis tools or data; Wrote paper. U.G.U.: Contributed reagents, materials, analysis tools or data; wrote paper. N.C.O.: Conceived and designed the experiment; Analyzed and interpreted data; wrote the paper. All authors read and approved the final manuscript.

**Funding**
We have not received any funding.

**Availability of data and materials**
It will be made available on request.

## Declarations

**Ethics approval and consent to participate**
The Animal Ethics Committee of the Faculty of Pharmaceutical Science, University of Nigeria, Nsukka approved the research protocol for the use of experimental animals. Hence, the study was conducted in accordance with the Ethical Guidelines of the Animal Care and Use Committee (Research Ethics Committee) of the University of Nigeria, Nsukka following the Federation of European Laboratory Animal Science Association and the European Community Council Directive (86/609/EEC).

**Consent for publication**
Not applicable.

**Competing interests**
The authors declare that they have no competing interests.

**Author details**
[1]Department of Pharmaceutical Technology and Industrial Pharmacy, University of Nigeria, Nsukka 410001, Nigeria. [2]Department of Pharmaceutics and Drug Production Evaluation, Roosevelt University, Schaumburg, IL, USA. [3]Department of Biochemistry, University of Nigeria, Nsukka, Nigeria.

Received: 29 January 2023 Accepted: 14 November 2023
Published online: 04 January 2024

**References**

1. Asghar AA, Akhlaq M, Jalil A, Azad AK, Asghar J, Adeel M, Albadrani GM, Al-Doaiss AA, Kamel M, Altyar AE, Abdel-Daim MM (2022) Formulation of ciprofloxacin-loaded oral selfemulsifying drug delivery system to improve the pharmacokinetics and antibacterial activity. Front Pharmacol 13:967106. https://doi.org/10.3389/fphar.2022.96
2. Rehman FU, Farid A, Shah SU, Dar MJ, Rehman AU, Ahmed N, Rashid SA, Shaukat I, Shah M, Albadrani GM et al (2022) Self-emulsifying drug delivery systems (SEDDS): measuring energy dynamics to determine thermodynamic and kinetic stability. Pharmaceuticals 15:1064. https://doi.org/10.3390/ph15091064
3. Hsieh CM, Yang TL, Putri AD, Chen CT (2023) Application of design of experiments in the development of self-microemulsifying drug delivery systems. Pharmaceuticals 16:283. https://doi.org/10.3390/ph16020283
4. Obitte NC, Ofokansi KC, Kenechukwu FC (2014) Development and evaluation of novel self-nanoemulsifying drug delivery systems based on a homolipid from capra hircus and its admixtures with melon oil for the delivery of indomethacin. J Pharm 2014
5. Anna CK, Marta S, Aleksandra A, Emilia S, Katarzyna W (2015) Development and evaluation of liquid and solid self-emulsifying drug delivery system for atorvastatin. Molecules 20:21010–21022
6. Patel PV, Patel HK, Panchal SS, Mehta TA (2013) Self micro-emulsifying drug delivery system of tacrolimus: formulation, in vitro evaluation and stability studies. Int J Pharm Investig 3:95
7. Sachan R, Khatri K, Kasture S (2010) Self-eumlsifying drug delivery system: a novel approach for enhancement of bioavalibility. Int J Pharm Tech Res 2:1738–1745
8. Obitte N, Ugorji O, Ezichi L, Ogbodo S, Onyishi V (2015) Ibuprofen self-emulsifying drug delivery system. WJPPS 4:887–899
9. Porter AJ, Edwards GA, Charman WN (1998) Formulation design and bioavailability assessment of lipidic self-emulsifying formulation of halofanitrine. Int J Pharm 167:155–167
10. Constantinides PP (1995) Lipid microemulsions for improving drug dissolution and oral absorption. Phys Biopharm Asp Pharm Res 12:1561–1572
11. World Health Organization: Guidelines for the treatment of Malaria. https://whqlibdoc.who.int/publications/2010/9789241547925,2010. Accessed 20 June 2016
12. Hiroshi A, Mikio T, Masahiro H (2005) The novel formulation design of self emulsifying drug delivery systems (SEDDs) type o/w microemulsion II: stable gastrointestinal absorption of a poorly water soluble new compound ER-1258 in bile-fistula rats. Drug Metab Pharmacokinet 20:257–267
13. Obitte NC, Ezeiruaku H, Onyishi V (2008) Preliminary studies on two vegetable based self emulsifying drug delivery systems (SEDDs) for the delivery of Metronidazole, a poorly water soluble drugs. J Appl Sci 8:1950–1955
14. Gaikwad SN, Lonare MC, Tajne MR (2020) Enhancing solubility and bioavailability of artemether and lumefantrine through a self-nano emulsifying drug delivery system. Indian J Pharm Sci 82:282–290

15. Obitte NC, Ofokansi KC, Chime SA, Idike E (2013) Solid self-emulsifying drug delivery system based on a homolipid and vegetable oil: a potential vehicle for the delivery of indomethacin a disadvantaged drug. Int J Green Pharm 7:244–251
16. Okorji UP, Velagapudi R, El-Bakoush A, Fiebich BL, Olajide OA (2016) Antimalarial drug artemether inhibits neuroinflammation in BV2 microglia through Nrf2-dependent mechanisms. Mol Neurobiol 53:6426–6443
17. Inciardi RM, Solomon SD, Ridker PM, Metra M (2020) Coronavirus 2019 disease (COVID-19), systemic inflammation, and cardiovascular disease. J Am Heart Assoc 9:e017756
18. Reyes AZ, Hu KA, Teperman J, Wampler Muskardin TL, Tardif JC, Shah B, Pillinger MJ (2020) Anti-inflammatory therapy for COVID-19 infection: the case for colchicine. Ann Rheum Dis 0:1–8
19. Achan J, Serwanga A, Wanzira H, Kyagulanyi T, Nuwa A, Magumba G, Kusasira S, Sewanyana I, Tetteh K, Drakeley C, Nakwagala F, Aanyu H, Opigo J, Hamade P, Marasciulo M, Baterana B, Tibenderana HK (2021) Current malaria infection, previous malaria exposure, and clinical profiles and outcomes of COVID-19 in a setting of high malaria transmission: an exploratory cohort study in Uganda. Lancet Microbe 3:e62-71
20. Patel K, Sarma V, Vavia P (2013) Design and evaluation of lumefantrine—oleic acid self nanoemulsifying ionic complex for enhanced dissolution. DARU J Pharm Sci 21:1–10
21. Kashif S, Sheikh R, Sadath A, Syed SI, Akhlaquer RG, Ahmad KJ, Farhan J (2017) Development and in vitro/ in vivo evaluation of artemether and lumefantrine co-loaded nanoliposomes for parenteral delivery. J Liposome Res 29:1–21
22. Gahoi S, Jain GK, Tripathi R, Pandey SK, Anwar M, Warsi MH (2012) Enhanced antimalarial activity of lumefantrine nanopowder prepared by wet-milling DYNO MILL technique. Colloids Surf B Biointerface 95:16–22
23. Djimdé A, Lefèvre G (2009) Understanding the pharmacokinetics of Coartem. Malar J 8(Suppl 1):1–8. https://doi.org/10.1186/1475-2875-8-S1-S4
24. Jain JP, Leong FJ, Chen L, Kalluri S, Koradia V, Stein DS, Wolf MC, Sunkara G, Koja J (2017) Bioavailability of lumefantrine is significantly enhanced with a novel formulation approach, an outcome from a randomized, open-label pharmacokinetic study in healthy volunteers. Antimicrob Agents Chemother 61:e00868-e917
25. Pereda M, Poncelet D, Renard D (2019) Characterization of core-shell alginate capsules. Food Biophys. https://doi.org/10.1007/s11483-019-09595-x
26. Mbah CC, Builders PF, Akuodor GC, Kunle OO (2012) Pharmaceutical characterization of aqueous stem bark extract of Bridelia ferruginea Benth (Euphorbiaceae). Trop J Pharm Res 11:637–644
27. Aulton ME (1999) Pharmaceutics: the science of dosage form design. Intl., Stud. Edinburgh, Churchill Livingstone
28. Peters W, Portus JH, Robinson BL (1975) The chemotherapy of rodent malaria. XXII, the value of drug-resistant strains of *P. berghei* in screening of blood Schizonticidal activity. J Trop Med Hyg 69:155–171
29. Schulman JH, Riley DP (1948) X-ray investigation of the structure of transparent oil-water disperse system. I. J Colloid Interface Sci 3:383
30. Fidock DA, Rosenthal SL, Croft SL, Brun R, Nwaka S (2004) Antimalarial drug discovery: efficacy models for compound screening. Nat Rev Drug Discov 3:509–520
31. Koffuor GA, Amoateng P, Andey TA (2011) Immunomodulatory and erythropoietic effects of aqueous extract of the fruits of Solanum torvum Swartz (Solanaceae). Pharmacogn Res 3:3130–3134
32. Agrawal S, Khadase S, Talele G (2010) Bioactive immunomodulatory fraction from Tridax procumbens. Asian J Biol Sci 3:120–127
33. Ó'Cconnell KE, Mikkola AM, Stepanek AM, Vernet A, Hall CD, Sun CC, Yildirim E, Staropoli JF, Lee JT, Brown D (2015) Practical murine hematopathology: a comparative review and implications for research. Comp Med 65:96–113
34. Bancroft JD, Gamble M (2002) Theory and practice of histological techniques, 5th edn. Churchill Livingston, Edinburgh
35. Gibson-Corley KN, Olivier AK, Meyerholz DK (2013) Principles for valid histopathologic scoring in research. Vet Pathol 50:1007–1015
36. Pallavi MN, Swapnil LP, Shradha ST (2012) Self emulsifying delivery system (SEDDs): a review. Int J Pharm Biol Sci 2:42–52
37. Mcclements D (2012) Nanoemulsions versus microemulsions: terminology, differences, and similarities. Soft Matter 8:1719–1729. https://doi.org/10.1039/C2SM06903B
38. Pouton CW (1985) Self-emulsifying drug delivery systems: assessment of the efficiency of emulsification. Int J Pharm 27:335–348
39. Wei L, Sun P, Nie S, Pan W (2005) Preparation and evaluation of SEDDS and SMEDDS containing carvedilol. Drug Dev Ind Pharm 31:785–794
40. BASF Technical Document on Kollidon VA 64. 2019. BASF—nutrition & health. www.pharma-ingredients.basf.com. Accessed 20 Feb 2022
41. Dinunzio JC, Hughey JR, Brough C, Miller DA, Williams RO, McGinity J (2010) Production of advanced solid dispersions for enhanced bioavailability of itraconazole using KinetiSol Dispersing. Drug Dev Ind Pharm 36:1064–1078
42. Majeed U, Hanif U, Ghulam M, Qaisar M, Izhar H (2015) Evaluation of influence of various polymers on dissolution and phase behavior of carbamazepine-succinic acid cocrystal in matrix tablets. Biomed Res Int 2015:1–10
43. Gershanik T, Benita S (1996) Positively-charged self-emulsifying oil formulation for improving oral bioavailability of progesterone. Pharm Dev Technol 1:147–157
44. Bauer E, Jakob S, Mosenthin R (2005) Principles of physiology of lipid digestion. Asian Aust J AnimSci 18:282–295
45. Carey MC, Hernell O (1992) Digestion and absorption of fat. Semin Gastrointest Dis 3:189–208
46. Tang B, Cheng G, Gu J, Xu C (2008) Development of solid self emulsifying drug delivery systems: preparation techniques and dosage forms. Drug Discov Today 13:606–612
47. Constantinides PP, Scalart J (1997) Formulation and physical characterization of water-in-oil microemulsion containing long-versus medium-chain glycerides. Int J Pharm 158:57–68
48. Mandawgade SD, Sharma S, Pathak S, Patravale VB (2008) Development of SMEDDS using natural lipophile: application to artemether delivery. Int J Pharm 362:179–183
49. Carter SJ (1986) Powder flow and compaction. In: Cooper and gun's tutorial pharmacy, 2nd edn. CBS Publishers and Distributors, India
50. Gebre-Mariam TA, Nikolayev AS (1993) Evaluation of starch obtained from Ensete ventricosum as a binder and disintegrant for compressed tablets. J Pharm Pharmacol 45:317–320
51. Obitte NC, Chukwu A, Onyishi IV, Obitte BCN (2009) The Physicochemical Evaluation and Applicability of Landolphia owariensis latex as a release modulating agent in its admixture with carbosil in Ibuprofen loaded Self Emulsifying Oil Formulations. Int J Appl Res Nat Prod 2:27–43
52. Okafor SI, Chukwu A (2003) The binding property of grewa gum II: some physical properties of sodium salicylate tablets. West Afr J Biol Sci 14:9–12
53. Kerc J, Srcic S (1995) Thermal analysis of glassy pharmaceuticals. Thermochim Acta 248:81–95
54. Agarwal V, Siddiqui A, Ali H, Nazzal S (2009) Dissolution and powder flow characterization of solid self emulsified drug delivery system (SEDDS). Int J Pharm 366:44–52
55. Kang MJ, Jung SY, Song WH, Park JS, Choi SU, Oh KT, Choi HK, Choi YW, Lee J, Lee BJ (2011) Immediate release of ibuprofen from fujicalin based fat dissolving self emulsifying tablets. Drug Dev Ind Pharm 37:1298–1305
56. Paradkar A, Patil P, Patil V (2007) Formulation of a self-emulsifying system for oral delivery of simvastatin: in vitro and in vivo evaluation. Acta Pharm 57:111–122
57. Neusilin Bronchure (2009) Fuji chemical industry co. Ltd. http://harke.com/fileadmin/images/pharma/fuji_Neusilin. Accessed 08 June 2016
58. Fujichemical News Letter (2007) https://www.fujichemical.co.jp/english/newsletter/newsletter_pharma_0710.html. Accessed 02 Feb 2022
59. Higuchi T (1963) Mechanism of sustained action medication: theoretical analysis of rate of release of solid drugs dispersed in solid matrices. J Pharm Sci 52:1145–1148
60. Rodriguez DP (2014) Formulation and preparation of niosomes containing bioactive compounds. Doctoral thesis, Universidad de Oviedo
61. Dannenfelser HH, Joshi Y, Bateman S, Serajuddin K (2004) Development of clinical dosage forms for a poorly water soluble drugs: application of polyethylene glucopoly sorbate solid dispersion carrier system. J Pharm Sci 93:1165–1175
62. Kanika S, Pawar YB, Arvind KB (2010) Self emulsifying drug delivery systems: a strategy to improve oral bioavailability. Curr Res Inf Pharm Sci 11:42–49
63. Nfambi J, Bbosa GS, Sembajwe LF, Gakunga J, Kasolo JN (2015) Immunomodulatory activity of methanolic leaf extract of *Moringa oleifera* in Wistar albino rats. J Basic Clin Physiol Pharmacol 26:603–611
64. Goronzy JJ, Weyand CM (2007) The innate and adaptive immune systems. In: Goldman L (ed) Cecil Medicine Saunders Elsevier Inc, Philadelphia
65. Carrillo CM, Del- Cavia M, Alonso-Torre S (2012) Role of oleíc add in immune system; mechanism of action; a review. Nutr Hosp 27:978–990

66. Pereira LM, Hatanaka E, Martins EF, Liberti FO, Farsky EA, Curi SH, Pithon-Curi R, Tania C (2008) Effect of oleic and linoleic acids on the inflammatory phase of wound healing in rats. Cell Biochem Funct 26:197–204
67. Puja M, Daniel FM, Michael B, Emilie S, Rachel ST, Jessica JM (2020) COVID-19: consider cytokine storm syndromes and immunosuppression. Lancet 395:1033–1034
68. Mohammad AC, Nayem H, Mohammod AK, Abdus S, Ashraful A (2020) Immune response in COVID-19: a review. J Infect Public Health 13:1619–1629
69. Aravinthan A, Verma S, Coleman N, Davies S, Allison M, Alexander G (2012) Vacuolation in hepatocyte nuclei is a marker of senescence. J Clin Pathol 65:557–560
70. Boampong JN (2015) In Vivo antiplasmodial, anti-Inflammatory, and analgesic properties, and safety profile of root extracts of *Haematostaphis barteri* Hook F. (Anacardiaceae). J Parasitol Res 2015:872892

## Publisher's Note